A Project Report on

ISLANDING OPERATION AND AUTONOMOUS POWER MANAGEMENT FOR INTERLINKED AC/DC MICROGRIDS

Submitted in partial fulfilment of the requirement for the award of degree of

BACHELOR OF TECHNOLOGY
IN
ELECTRICAL AND ELECTRONICS ENGINEERING

By

K. Divakar (19985A0231) **M. Anjali (19985A0242)**

T. Sai Ganesh(19985A0290) **Y. DileepPrudhvi(19985A0298)**

Under the guidance

of

Mr. P. Srinivas

Assistant Professor

DEPARTMENT OF ELECTRICAL AND ELECTRONICS ENGINEERING
RAGHU ENGINEERING COLLEGE
Accredited by NBA, NAAC 'A' Grade, Permanently Affiliated to JNTUK
Dakamarri (V), Bheemunipatnam (M), Visakhapatnam Dist, Andhra Pradesh-531162

2021 – 2022

ISLANDING OPERATION AND AUTONOMOUS POWER MANAGEMENT FOR INTERLINKED AC/DC MICROGRIDS

A ISLANDING OPERATION AND AUTONOMOUS POWER MANAGEMENT FOR INTERLINKED AC/DC MICROGRIDS

is

Submitted in partial fulfillment of the requirements for the award of the degree of

Bachelor of Technology

in

DEPARTMENT OF ELECTRICAL AND ELECTRONICS ENGINEERING

by

Project Batch

K. Diwakar	**19985A0231**
M. Anjali	**19985A0242**
T. Sai Ganesh	**19985A0290**
Y. Dileep Prudhvi	**19985A0298**

Under the Guidance of

Mr. P. Srinivas
Assistant Professor

RAGHU ENGINEERING COLLEGE (Autonomous)
Accredited by NBA, NAAC 'A' Grade, Permanently Affiliated to JNTUK
Dakamarri (V), Bheemunipatnam (M), Visakhapatnam Dist, Andhra Pradesh-531162

2021 – 2022

RAGHU ENGINEERING COLLEGE (Autonomous)

Department of Electrical and Electronics Engineering

CERTIFICATE

It is certified that the work contained in the project report titled "**ISLANDING OPERATION AND AUTONOMOUS POWER MANAGEMENT FOR INTERLINKED AC/DC MICROGRIDS**," by

K. Diwakar	**19985A0231**
M. Anjali	**19985A0242**
T. Sai Ganesh	**19985A0290**
Y. Dileep Prudhvi	**19985A0298**

has been carried out under my/our supervision and that this work has not been submitted elsewhere for a degree.

(Digital Signature)
Signature of the Project Guide
P. Srinivas
Assistant Professor

(Digital Signature)
Signature of HOD
P. Sasi Kiran
Department of EEE

Signature of the External Examiner

Date:

DECLARATION

We hereby declare that the project entitled "**ISLANDING OPERATION AND AUTONOMOUS POWER MANAGEMENT FOR INTERLINKED AC/DC MICROGRIDS**" submitted for the fulfilment of B. Tech. (EEE) the degree is our original work and the project report has not formed the basis for the award of any other degree, diploma, fellowship or any other similar titles. I also declare that the ideas/sources used in the preparation of the document are adequately cited and referenced the sources.

Student Signatures

K. Divakar (19985A0231)

M. Anjali (19985A0242)

T. Sai Ganesh (19985A0290)

Y. Dileep Prudhvi (19985A0298)

Date:

ACKNOWLEDGEMENT

We are grateful to Mr. P. Srinivas, Assistant Professor, Department of EEE for assigning us the project and for his guidance. We would definitely like to record thanks for his constant support. His Persisting encouragement, everlasting patience and keen interest in discussions have benefited us to the extent that cannot be spanned by words. He has been the continuous source of inspiration for us throughout the work. We would extend our thanks for his constructive criticism without which the project would not have taken the shape.

We are extremely thankful to Mr. P. Sasi Kiran, Professor and Head of the EEE-Department for extending his co-operation, suggestions and keenness in the completion of this project work.

We are greatly thankful to Dr. Ch. Srinivasu -Principal, for the valuable suggestions and continuous encouragement provided to us in the completion of project work.

We would express our deep sense of gratitude to Dept. of Electrical and Electronics Engineering for providing us the opportunity for project and providing all the necessary resources and expertise for this purpose. We are grateful to our parents for their everlasting support and encouragement in all walks of our lives.

ABSTRACT

The existing power management schemes for interlinked AC-DC micro grids have several operational drawbacks. Some of the existing control schemes are designed with the main objective of sharing power among the interlinked micro grid on their loading conditions, while other schemes regulate the voltage of the interlinked micro grids without considering the specific loading conditions. However, the existing schemes cannot achieve both objectives efficiently. To address these issues, an autonomous power management scheme is proposed, which explicitly considers the specific loading condition of the DC micro grid before importing power from the interlinked AC micro grid. This strategy enables voltage regulation in the DC micro grid, and also reduces the number of converters in operation. The proposed scheme is fully autonomous while it retains the plug-n play features for generators and tie-converters. The performance of the proposed control scheme has been validated under different operating scenarios. The results demonstrate the effectiveness of the proposed scheme in managing the power deficit in the DC micro grid efficiently and autonomously while maintaining the better voltage regulation in the DC micro grid. The results are verified through MATLAB/SIMULINK environment.

CONTENTS

CHAPTER 1: INTRODUCTION **1-4**
1.1 Overview 1-2
1.2 Literature survey 2-3
1.3 Objective of the work 4

CHAPTER 2: MODELLING OF PHOTOVOLTAIC SYSTEM **5-15**
2.1 Introduction 5-6
2.2 Photovoltaic Generation 6
2.3 Solar Irradiance 7-9
2.4 PV cell characteristic 9-11
2.5 Maximum Power point 11-12
2.6 Photovoltaic system model 13-15

CHAPTER 3: MICRO GRIDS **16-21**
3.1 Architecture of Micro grid 16-17
3.2 Classification of Micro grid 17-18
3.3 DC Micro grid 18-19
3.4 AC Micro grid 19
3.5 AC/DC Micro grid 19-20
3.6 Importance of Microgrid 20-21

CHAPTER 4: AC-DC CONVERTER **22-27**
4.1 Introduction 22
4.2 Single phase fully controlled half wave rectifier 23-26
4.3 Single phase fully controlled bridge rectifier 26-27

CHAPTER 5: PROPOSED TOPOLOGY **28-33**
5.1 Control Strategies 28-29
5.2 Proposed hybrid control of Tie-converters 30-32
5.3 Performance validation 32-33

CHAPTER 6: CONTROLLERS AND PWM TECHNIQUES **34-41**
6.1 Introduction 34
6.2 Proportional controller 34-35
6.3 Integral controller 35-36
6.4 Derivative controller 36
6.5 Proportional and Integral controller 37-38
6.6 Modulation Techniques 38
6.7 Types of Modulation Strategies 38-41

CHAPTER 7: MATLAB DESIGN AND SIMULATION RESULTS **42-51**
7.1 Introduction of MATLAB 42

7.2 Simulink 43
7.3 Continuous and Discrete systems 44
7.4 Mathematical operations 44-45
7.5 Signals and Data transfer 45
7.6 Setting simulation parameters 46
7.7 Simulation diagrams and results 47-51

CONCLUSION **52**

REFERENCES **53-54**

CHAPTER-1

INTRODUCTION

1.1 Over View:

The technical advancement in power electronics is playing an important role in the deployment of renewables and alternative energy technologies which have so far been widely realized in different forms of network topologies and configurations. Similarly, they have been controlled and managed using various control strategies and architectures. Their network topologies and control strategies are mainly determined to maximize the benefits while meeting the load requirements. At present, renewable and alternative energy technologies are widely deployed in micro grids. The deployment of these new technologies in the form of a micro grid is preferred due to several advantages, such as optimal utilization of resources, improved power quality and enhanced supply reliability. Recently, more advanced grid architectures have emerged including the zone-based grid architecture, multi-micro grids, interlinked AC-AC micro grids and interlinked AC-DC micro grids. The main objective of these advanced network architectures is to exploit maximum benefits from renewable and alternative energy resources. For example, by interconnecting two or more micro grids, it will enable reserve sharing, support voltage and frequency, and ultimately enhance the overall reliability and resilience of interlinked micro grids. The interlinking arrangement between two or more microgrids or with utility grids primarily depends on the overall objectives, as well as the control and management scheme used in individual micro grids. The micro grids can be interlinked directly or through harmonizing tie converters. The harmonizing tie-converters are primarily used when two or more microgrids have different operating voltages and/or frequencies. The tie converters are also essential if the microgrids to be interlinked have different control strategies and the power flow among them needs to be regulated.

Similarly, the interlinking of the DC microgrid with the utility grid or another AC microgrid Also requires tie-converters to regulate the power flow among other functionalities, and that has been investigated under various scenarios in the published literature. In, the demand-droop control has been proposed for the interlinking or tie-converters of the AC-DC microgrids. The power flow action is determined based on the normalized terminal voltage and frequency of the droop controlled interlinked AC-DC micro grids. This scheme enables

autonomous power transfer between two interlinked micro grids based on their relative loading condition. The power flow decision based on the relative loading may cause the interlinking converter to operate continuously, and thus it may result in unnecessary operational losses. The same power sharing scheme has been extended to interlinked microgrids with a storage system.

This scheme is further improved with the progressive auto-tuning to minimize the energy flow through interlinking converters. The proposed auto-tuning enables the power transfer only when one micro grid is heavily-loaded, and another micro grid is lightly-loaded. The droop-based power sharing concept has been further investigated for different operating conditions of the interlinked AC and DC micro grids In, the power management strategy is presented for a three-port system comprising AC, DC and a storage network. The decision about the power sharing is based on the loading con-So far, the published decentralized power sharing schemes for interlinked AC-DC microgrids are either entirely based on droop principle or voltage regulation. The droop-based power sharing schemes transfer power based on relative loading of all converters will operate regardless of the overall power transfer requirement. This may incur unnecessary converter operational losses. Contrarily, the voltage regulation schemes regulate the voltage of the DC microgrid without considering specific loading conditions of the generators, and lacks the plug-n-play feature for tie-converters. These shortcomings can be specifically addressed using the proposed control scheme in this project.

1.2 Literature Survey:

J. Rocabert, A. Luna, F. Blaabjerg, and P. Rodr´ıguez, "Control of power converters in AC microgrids," IEEE Transactions on Power Electronics" proposed the enabling of ac microgrids in distribution networks allows delivering distributed power and providing grid support services during regular operation of the grid, as well as powering isolated islands in case of faults and contingencies, thus increasing the performance and reliability of the electrical system. The high penetration of distributed generators, linked to the grid through highly controllable power processors based on power electronics, together with the incorporation of electrical energy storage systems, communication technologies, and controllable loads, opens new horizons to the effective expansion of microgrid applications integrated into electrical power systems.

This project carries out an overview about microgrid structures and control techniques at different hierarchical levels. At the power converter level, a detailed analysis of the main operation modes and control structures for power converters belonging to microgrids is carried out, focusing mainly on grid-forming, grid-feeding, and grid-supporting configurations. This analysis is extended as well toward the hierarchical control scheme of microgrids, which, based on the primary, secondary, and tertiary control layer division, is devoted to minimize the operation cost, coordinating support services, meanwhile maximizing the reliability and the controllability of microgrids. Finally, the main grid services that microgrids can offer to the main network, as well as the future trends in the development of their operation and control for the next future, are presented and discussed.

M. Liserre,T. Sauter, and J. Y. Hung, "Future energy systems: integrating renewable energy sources into the smart power grid through industrial electronics," This project proposes a single-stage inverter system with maximum power point tracking control (MPPT) applicable in low-power photovoltaic (PV) energy conversion systems. The proposed system is successfully implemented using a single digital signal processor (DSP) TMS320F2808.

The proposed single-stage inverter system has the following features: 1) the ability to harvest the maximum PV power using two simple and effective current sampling methods; 2) flexible topology based on the positioning of DC link capacitor on the outside of the inverter bridge circuits; 3) reduced volume and higher efficiency than the conventional two-stage inverters, and 4) MPPT accuracy of 99.3% with overall efficiency of 90% under the full-load condition.

T. Strasser, F. Andren, J. Kathan, C. Cecati, C. Buccella, P. Siano, P. ´ Leitao, G. Zhabelova, V. Vyatkin, P.Vrba, and V. Marık, "A review of architectures and concepts for intelligence in future electric energy systems," The main theme of this scheme is to regulate the power among the interlinked microgrids by considering a specific loading condition. This autonomous power management scheme for interlinking microgrids considers a specific loading condition of dc micro grid before importing power from Ac micro grid by using an interlinking through a medium called three-level inverter. The use three-phase three level inverters can reduce the harmonic distortion in the output waveform without any filter circuit and also operates for higher and lower switching frequencies.

1.3 Objective of the Work:

The proposed autonomous power management scheme for interlinked AC-DC micro grids takes into consideration the specific loading condition of the generators, and transfers power from AC to DC micro grid during its peak-load demand, and also regulates the voltage of the DC micro grid. The proposed scheme enables the plug-n-play feature for tie converters and reduces the number of converters in operation to avoid unnecessary losses. In the considered scenario, the DC micro grid has inadequate generation capacity due to the high variability of the loads and renewable generation. The AC micro grid is considered to have regulated voltage and frequency as well as the surplus power to transfer to the DC micro grid during its peak demand or contingency condition. To achieve the features discussed above, a hybrid droop and voltage regulation mode control has been proposed for the tie-converters in interlinked AC-DC microgrids.

The proposed control scheme relies on the tie-converter terminal voltage information to determine the overall loading condition of the droop-controlled DC microgrid. Based on the set loading threshold, the tie-converter starts automatically and transfers power to the DC microgrid during the peak-load demand or contingency condition in the DC microgrid. With the proposed hybrid control mode, the voltage of the DC microgrid is regulated at a defined nominal level. In addition, the proposed scheme allows interfacing more than one tie-converters, but as opposed to the existing scheme where all tie-converters operate simultaneously regardless of the power transfer demand.

CHAPTER-2

MODELLING OF PHOTO VOLTAIC SYSTEM

2.1 Introduction

Greenhouse gasses rise throughout the lower atmosphere as both a consequence of human activities. Those of the sciences already agree that such a rise of carbon dioxide (CO2), methane (CH4) and other greenhouse gases induces a spike of world temperature which could contribute to much more global warming throughout the century. This increases the amount of greenhouse gasses. Safe and economically sustainable, clean electricity options. We will offer other economic immediate gains by reducing greenhouse gas pollution and therefore can help maintain natural fuels for potential forms of energy. The usage of solar cells to transform energy from solar irradiance through electricity is really a process that renewable support. The latest area of considerable business and academic concern becomes PV energy production. Recent research has also shown that PV generation is economically so desirable in the medium to longer term that it can be commonly adopted in many areas of the developing world. The introduction of a broad variety of distributed power generators would have far-reaching impacts both on delivery networks and on the regional transmission and generation structures. The balance is in the industrial centre, and electrically near to loads, because the PV generators are built on the buildings' roofs and sides. Such PV generators could, on the other side, be vulnerable to specific modes that may trigger a significant part of the working PV power to abruptly or rapidly detach.

The following failures were identified:

• Embedded generation (for example PV units) is normally fitted with protection devices for disconnection from either the network throughout the case of lack of control.

When there is a significant perturbation (for example the tripping of both the DC connection towards France or perhaps a big traditional generator), these safety schemes may trigger a large proportion of PV generation to also be turned off unexpectedly. Because this disconnection will be compounded by the initial disturbance, it may have severe repercussions.

• Even the high voltage output power of the pv generator systems may be momentarily disturbed by significant disruption. The whole perturbation could not be handled by the controller of the inverters that interface these PV components only with grid system. We can either malfunction or trigger the inverter to be shut down.

• A vast number of photovoltaic generators are expected to be found in crowded metropolitan areas. A moving, fast-moving weather front will reduce the irradiance from its highest value across such a region even below the minimum needed for the activity including its PV units in some kind of a matter of seconds.

2.2 Photovoltaic Generation

Light energy is being transformed to electricity by photovoltaic (PV) devices. The word picture means "moon" in Greek. "Volt" is called the Pioneer with Electricity Studies, Alessandro Volta (1745-1827). PV can mean "warm electricity," literally**".**

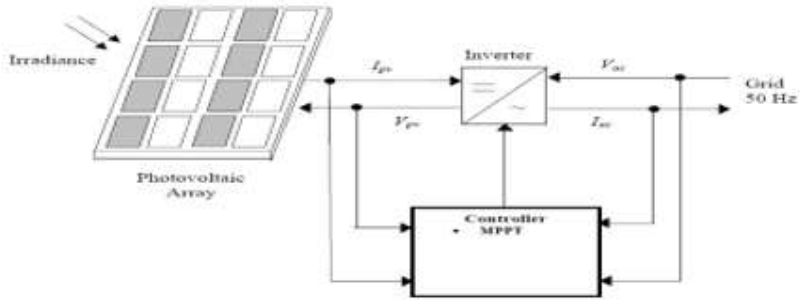

Figure: 2.1: Basic Configuration of Grid Connected PV Generation

Sunlight is transformed directly into ac power through a grid powered PV network. The program is primarily intended to reduce imports of energy from the power plant. Figure. 2.1 shows the simple grid-connected PV network configuration operating diagram. That PV's dc output was transformed through ac by means of an inverter. Each inverter function applies the whole central regulation: maximum power point monitoring (maximum power point tracking (MPPT).

2.3 Solar Irradiance

Sunlight is the reflective energy event on either a surface per unit of time. Normally in w / m2 it's also conveyed. That flow rate with electromagnetic energy becomes radiant power.

Sunlight comprises from electro-magnetic waves with photons, that travel at continuous motion, of various energies. Solar radiation of wavelength (μ) becomes inversely proportional towards photon intensity (E) Wave-like feature**.**

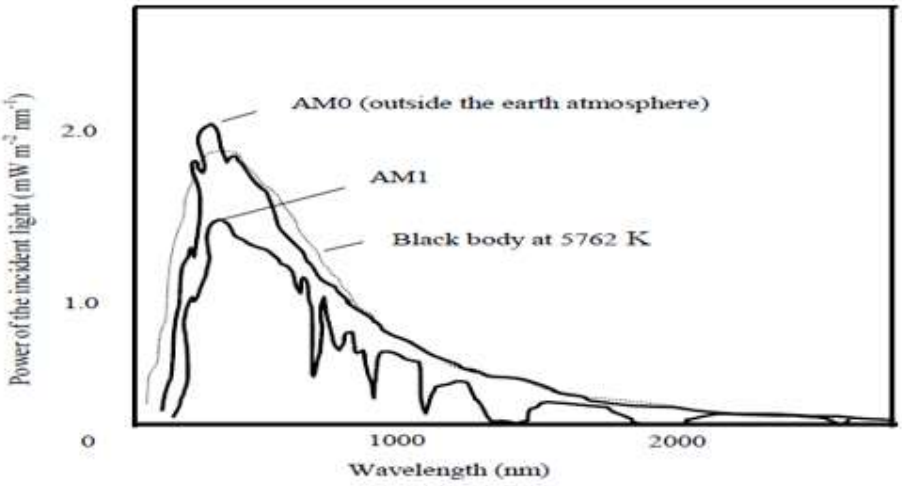

Figure: 2.2- The Spectrum of Sunlight

Fig.**2.2** shows the spectrum of the sun. At the temperature of **5762** K that illumination from either the sun is below the illumination from some kind of black eye. At this altitude, that dotted line indicates black body radiation. These are aligned with both the AM**0** curve that demonstrates the range of the sun at just the typical earth-sole gap beyond the Earth's atmosphere on either a perpendicular axis. The power intensity beyond the atmosphere of the planet is **1367** W / m**2** as well as the sun is continuously recognized. Air mass relates to the total spread across the surface of both the direct sunlight tube. If the sun will be at its height (opposite the global surface), the path of the light through the air is most limited, the path duration is **1.0 (**AM **1.0)** which helps to ascend to AM**1.** The light is obviously not even at the height in general. Its air pressure is heating up enough that but at bottom of **48.2** ° the air layer extends from either the sun's peak.

The energy intensity outside of the atmosphere of the planet is **1367** W / m**2**, and that this is considered the solar standard. Air mass relates to the proportional path length by the environment of the strong solar ray. Whenever the sun will be at its zenith (perpendicular to both the core of the universe). The direction is **1.0 (**AM **1.0)**, which ultimately leads to either the continuum of AM**1.** The trajectory in the atmosphere becomes shortest. The sky isn't quite at just the zenith, of course. As even the sun angle decreases with the zenith, their air

mass rises such that, at such a **48.2** ° angle, their air mass becomes **1.5** and even at a **60** ° angle their air mass becomes **2.0** as illustrated in Fig.**2.3.** AM **1.5** was accepted as the normal terrestrial illumination range**.**

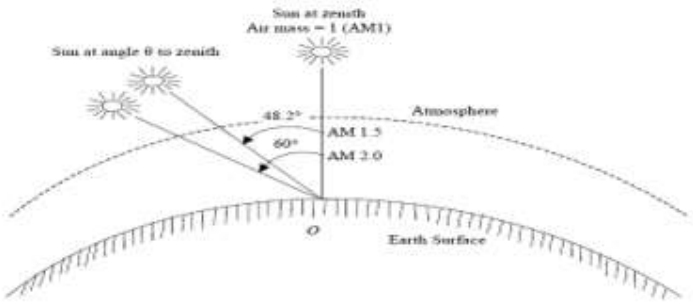

Figure: 2.3: Air mass concept

That PV inverter maximum output is typically estimated during sunlight AM1.5 (1kW / m2) with such a connective temperature of 25 ° C. It is the so named STC. That is the STC.

The principal explanation for the fluctuation with PV systems production capacity is the seasonal variation of solar irradiance due to the passing of clouds across a PV field. There are ten recorded weather types, with the greatest variability in the production strength in PV systems attributed towards cumulus clouds (puffy nuclei appearing like huge cotton balls) and squall lines (a straight line for black clouds). Square lines will carry a PV device performance down to zero, contributing with the worst-case scenario for machine service. Squall lines are therefore reliable, and it is possible to estimate the amount of time after which the PV network is out of operation. Cumulus clouds, from the other side, lead to reduced PV power loss, however they contribute to a more fluctuating PV performance because the irradiance fluxes when the clouds travel. Prevailing wind speed, form and scale of moving clouds as well as the region covered either by pv device and its topology, that time span of variations will vary from very few seconds to days.

Most frequently instead of not under twelve irradiance rates the most significant shifts in production capacity of PV systems happen. This duration often corresponds with the electrical system's off-top stacking time and therefore the operating entry point of both the PV process is most important. The magnitude of both the variances throughout PV force on the power network is controlled by some components such as the form of mists, penetration

degree including PV framework thickness, PV frame placement, System is supposed topology, etc.

The solar energy can usually be divided into two components:

1) Deterministic component identified in a given location either by regular, monthly, yearly environment and 2) stochastic component which contains the fluctuations of the probabilistic component but is decided by the everyday weather. If the predicted PV device performance energy is also to be measured over a certain amount of time, whether another deterministic irradiance portion or even the hourly emission details could be used. When, indeed, the efficiency and effect of PV systems mostly on electrical network needs to be investigated, therefore the resolution period for both the irradiance data will be as large as possible to avoid short-term or short-hour irradiance variations (variations of one hour). Moreover, high-temporal resolution surface temperature data (e.g., 10-minute resolution) will result in improved precision forecasts as the coefficients of self-correlation might have higher good attributes than those derived from 1-hour time resolution data.

2.4 Pv Cell Characteristic

Each PV cell is seen in Fig.2.4 throughout the analogous circuits defined by Eon (2.1).

$$I_{pv} = I_p - I_D - I_{sh} \qquad (2.1)$$

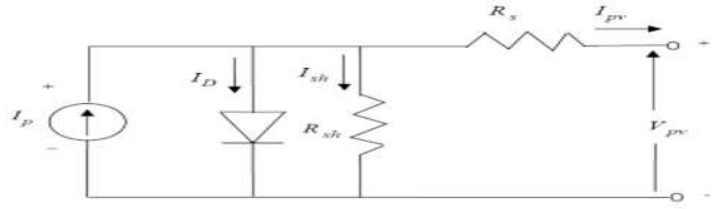

Figure: 2.4: PV Cell Equivalent Circuit

Figure: 2.5: Characteristic of PV Cell

Image. The operational function for Ivy – Vivo is seen in 2.5 for a PV unit. That quantity with PV cells is combined in order to obtain the necessary peak power level. By increase that voltage of even an individual cell by both the number of cells involved and by doubling that current by both the number of cells connected in parallel, that standard for the PV cluster may well be controlled. Under Fig.2.6, three main subjects of research should be noted**.**

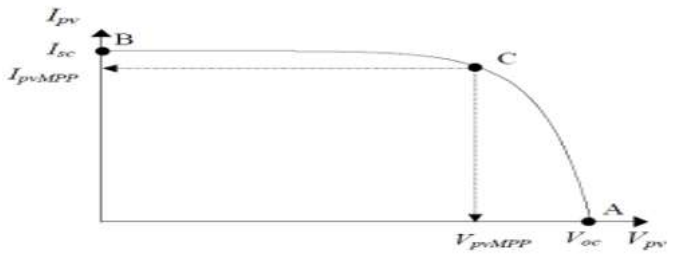

Figure: 2.6: PV Cell Operating Point

Open Circuit Voltage

As shown in fig.2.6 above, a point A.Figure.2.7 that open circuit voltage indicates that open circuit state where shunt voltage is overlooked. That mathematical argument, as seen in Eon (2.2) could be used to speak to**.**

$$I_p = I_0 \left[e^{\frac{qV_{oc}}{nkT}} - 1 \right] = 0$$

$$V_{OC} = \frac{nkT}{q} ln \left[\frac{I_p + I_0}{I_0} \right] \qquad (2.2)$$

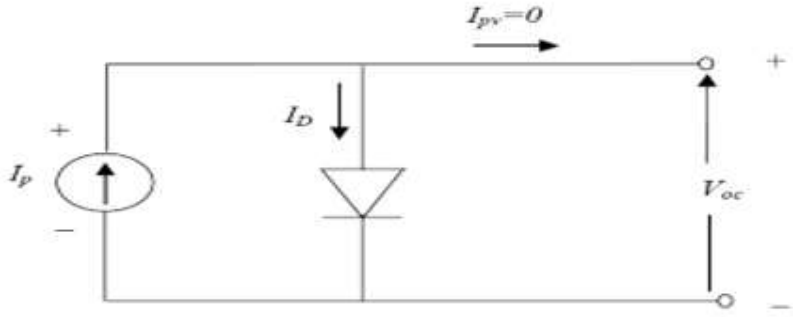

Figure: 2.7: Open circuit condition

Short Circuit Current: Present around point B as can be seen in Fig. 2.6 seems to be the value of the short circuit. Fig.2.8 reveals that the sequence resistance Rs have been ignored. Eon (2.3) may be portrayed.

$$I_{sc} = I_p \qquad (2.3)$$

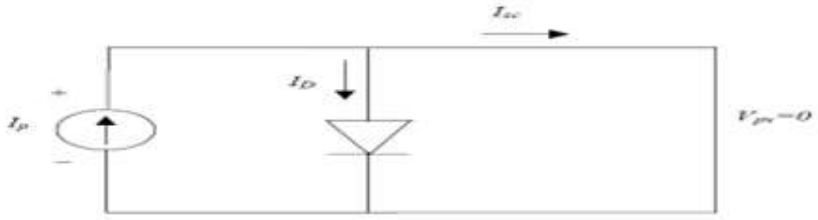

Figure: 2.8: Short Circuit Condition

2.5 Maximum Power Point

Each operating point of such a PV system is calculated either by intersection including its I_{pv}-V_{pv} function as well as the load function as seen in fig. Within continuous irradiance but cell temperature. 2.9. The feature of the loading is the line M=1 / R = Iliad / Load gradient. While the typical curve of both the I_{pv}-V_{pv} PV panel raises loading resistance between zero towards infinity, the device operating point shifted between B and A. The average working assignment is location c. It is equal to the average power consumption in the region belonging to the I_{pv}-V_{pv} function curve.

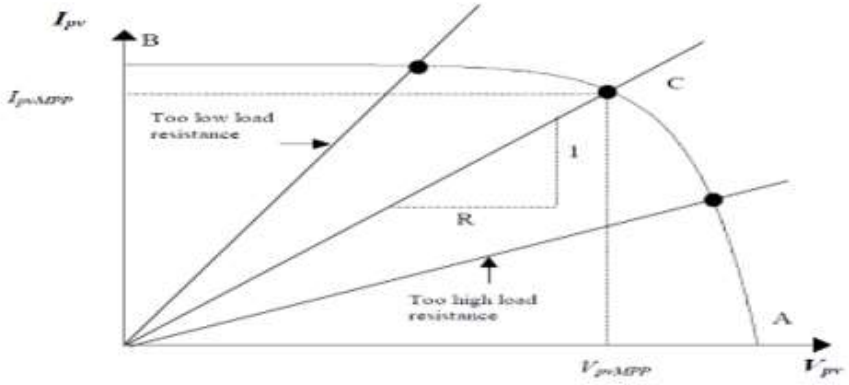

Figure: 2.9: Intersection of the I_{pv}-V_{pv} characteristic curve and the load characteristic

The operational points with in ca areas would have been if the load resistance became too strong. Operating points throughout the CB regions will be if maximum power was too small. The maximum production power, thus. The operational points could be in the CA sectors if another maximum power were too strong. The operation points throughout the areas CB would have been if the maximum power is too small. The optimum power point could therefore be reached by changing the voltage level to the PV array settings.

Effect Of Irradiance and Cell Temperature

Figs 2.10 & 2.11 simultaneously demonstrate the influence of radiation and temperature difference mostly on I_{pv}-V_{pv} curve. Image. 2.10 demonstrates that irradiance variates almost sequentially in maximal power consumption. Image. 2.11 indicates that since the water increases, the average array production capacity declines.

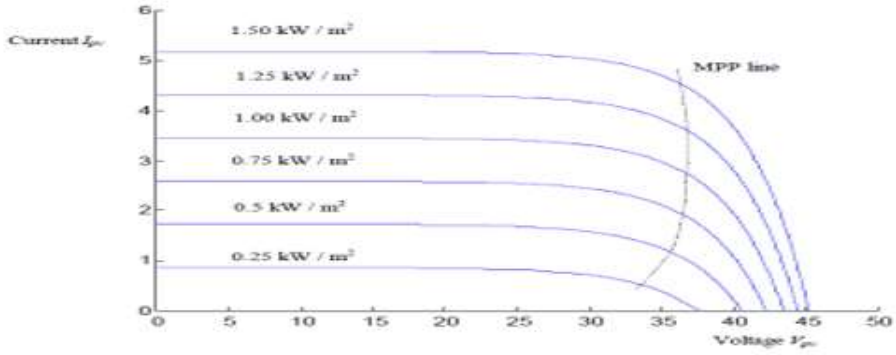

Figure: 2.10: Effect of irradiance on the I-V characteristic at constant cell temperature

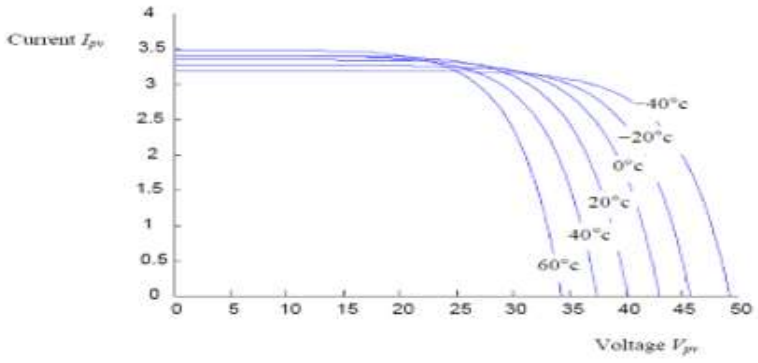

Figure: 2.11: Effect of temperature on the I-V characteristic at constant irradiance

2.6 Photovoltaic System Model

Figure shows the scheme diagram of a three-phase solar system with a grid attached, which would be the subject of this study. The 2nd December. That pv-system comprises a PV module, a DC-link C, a three-phase inverter as well as an L-filter inductor and therefore is linked by ea, eb as well as e_{ke} only with grid voltage.

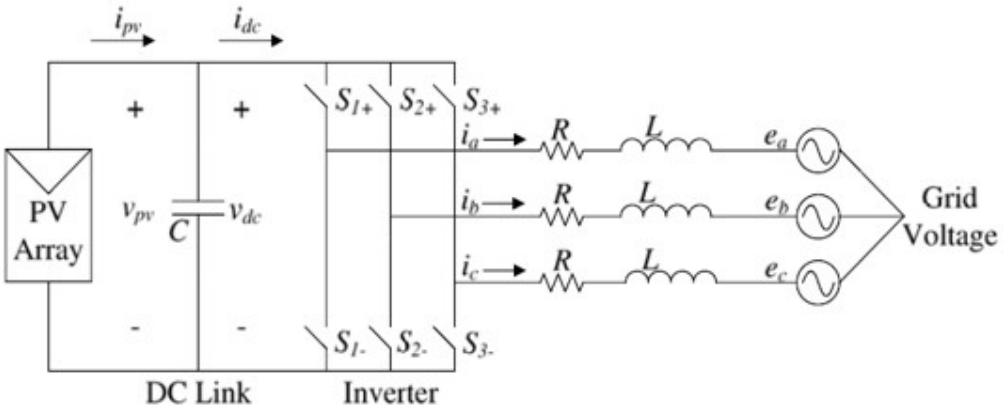

Figure: 2.12: Three-phase grid-connected PV system

Photovoltaic Cell and Array Modelling

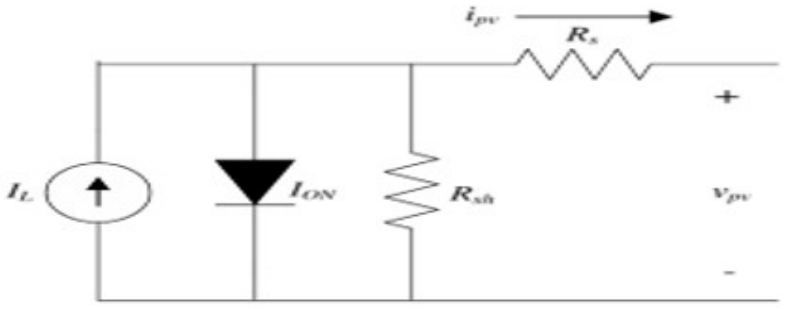

Figure: 2.13 Equivalent circuit diagram of PV cell

The p-n junction diode that converts the solar energy into electricity is indeed a basic p-n cell. Image. 2.13 display the corresponding circuit diagram of either a PV cell consisting of even an IL current background light, a parallel diode, a Rash shunt as well as a R_s resistance.

$$I_{ON} = I_s = \left[exp\left[\alpha\left(v_{pv} + R_s i_{pv}\right) - 1\right]\right] \qquad (2.4)$$

When α = q / Act, k = 1.3807 ~ 10−23 J.K−1 is constant, q = 1.6022 − 10−19 C becomes electron charge, it also is the optimal p-n crossover factor whose meaning varies from 1 to 5, Sattorial current but living power of the pv array are the output voltage, i.e., d.c., this really is the voltage over C.

Therefore, the latest law (KCL) by Kirchhoff is applied in Figure. 2.12, PV cell produced output current ivy could be written by

$$i_{pv} = I_L - \left[exp\left[\alpha\left(v_{pv} + R_s i_{pv}\right) - 1\right]\right] - \frac{v_{pv}+R_s i_{pv}}{R_{sh}} \qquad (2.5)$$

That current IL produced by light produced by the solar energy that can be connected by the:

$$I_L = \left[I_{sc} + k_i\left(T_c - T_{ref}\right)\right]\frac{s}{1000} \qquad (2.6)$$

Throughout the case of Isc, that current in either an open circuit is really the operating temperature of both the cell through Kelvin, s becomes solar irradiation, ki is the present coefficient of both the cell but Tref seems to be the relative temperature coefficient. That saturation current of a cell is responsible for the following formula to the temperature [19]:

$$I_s = I_{Rs}\left[\frac{T_C}{T_{Ref}}\right]^3 exp\left[\frac{qE_q}{Ak}\left(\frac{1}{T_{ref}} - \frac{1}{T_C}\right)\right] \qquad (2.7)$$

Using Erg is really the strength of both the band distance throughout the cell's half-conductor, and IRS seems to be the reverse cell digital evidence at comparison both solar irradiation temperatures. Because PV cells have very voltage drop, multiple PV cells in sequence are linked together to reach higher voltages. Thus, defend against harsh conditions and construct the PV panel, a collection of PV cells is mounted and encapsulated in glass, plastic, including other translucent materials. A variety of components are attached to build the PV array throughout parallel to achieve the necessary voltage and electricity.

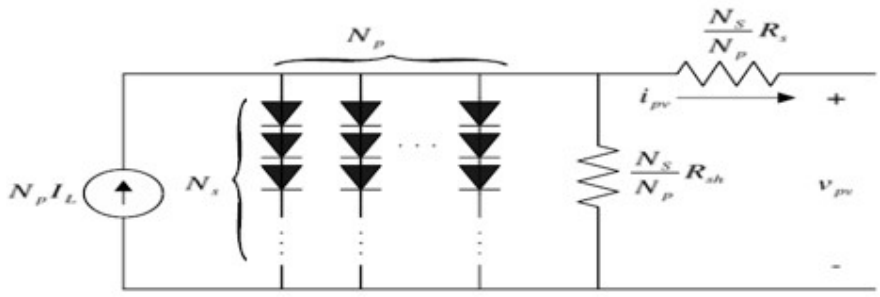

Figure: 2.14. Equivalent circuit diagram of PV array

Image. 2.14 illustrates that PV Array's electrical circuit analog diagram whereby Ns will be the quantity with series cells while Np their parallel number including its modules. That ipv list may be accessed in this situation

$$i_{pv} = N_P I_L - N_P I_s \left[exp \left[\alpha \left(\frac{v_{pv}}{N_s} + \frac{R_s i_{pv}}{N_P} \right) \right] - 1 \right] - \frac{N_P}{R_{sh}} \left(\frac{v_{pv}}{N_s} + \frac{R_s i_{pv}}{N_P} \right) \qquad (2.8)$$

PV systems were classified in three groups as per IEEE Standard 929-2000: 1) simple programs with a limit of 10 kW less than; 2) moderate systems with a range of 10 kW towards 500 kW; including 3) wide systems with a range over 500 kW. Nonetheless, the power levels of large devices newly built or scheduled for deployment are likely to change in the immediate future.

CHAPTER-3

MICRO GRIDS

3.1 Architecture of Micro grid:

Due to rise of concern for climate change and energy security. DG has receiving enormous popularity. Increasing fear of public perception in decreasing the carbon emission and due to acceptable liberalization of electricity market, there is the rise in the use of DG. The Micro grid concept involves a small transmission and distribution network that effectively make use of Distributed Energy Resource .

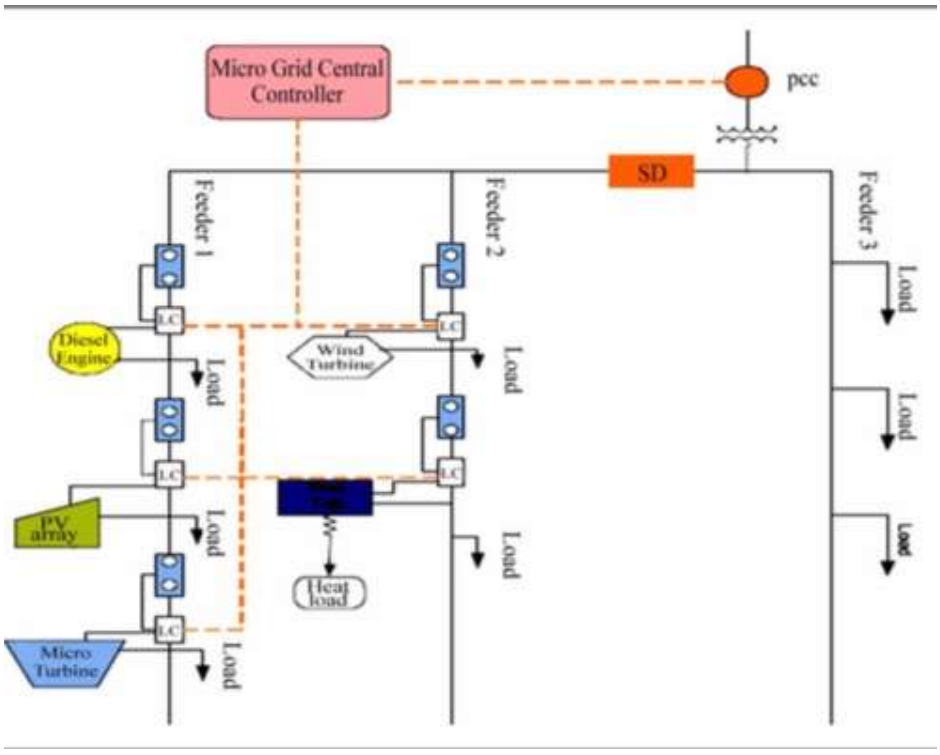

Figure 3.1- Architecture of Micro grid

Figure 3.1 shows the basic architecture of a micro grid. Here the micro grid is assumed to be radial with three feeders and some loads. Micro grid system is operated at a low voltage and it consists of several distributed energy resources such as solar panel, wind turbine, micro turbine and various energy storage devices such as flywheel, battery, super capacitors etc. Lay out of micro grid is shown in figure 2.2 which consists of power

transmission line, Communication, Protection equipment, point of coupling (PCC) and storage batteries along with loads.

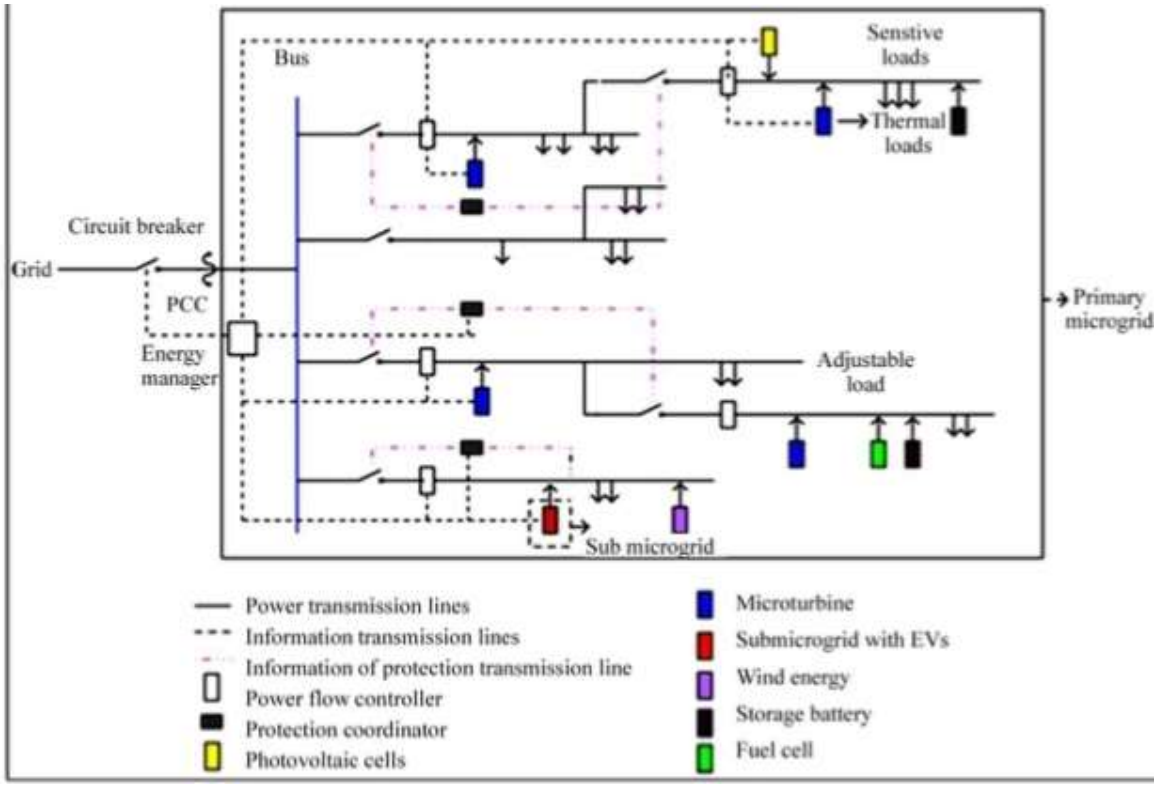

Figure 3.2- Microgrid Layout

Microgrid can operate in two modes: 1. Grid connected mode 2. Islanded mode

3.2 Classification of Microgrid:

Microgrids, classified as follows and studied from figure 2.3

i) Mode of operation

ii) Types

iii) Source

iv) Scenario

v) size

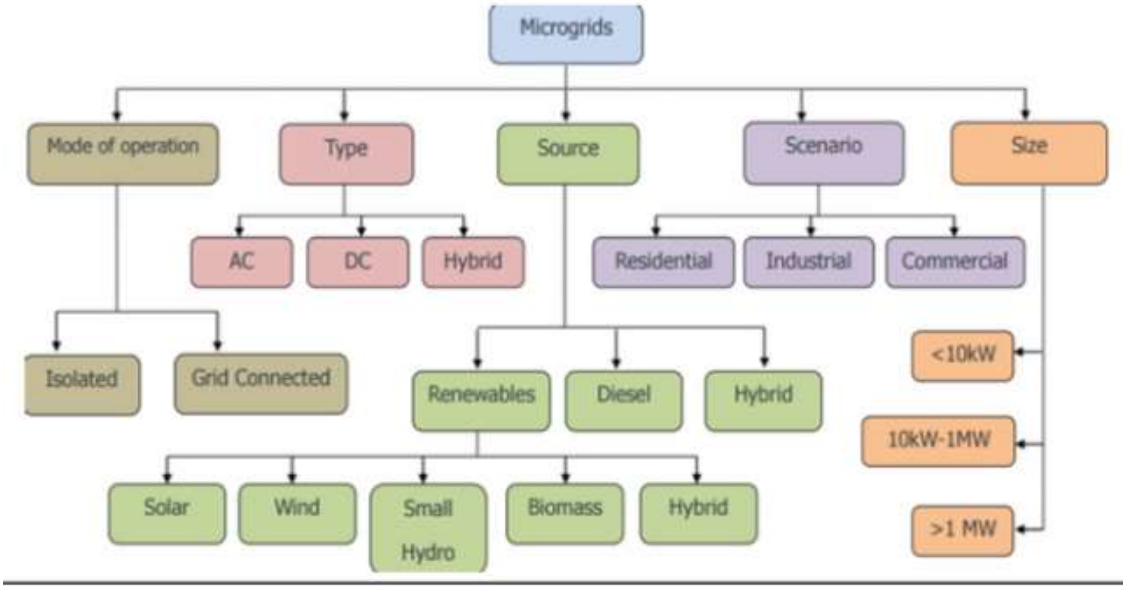

Figure 3.3- Classification of Micro Grid

3.3 DC Microgrid:

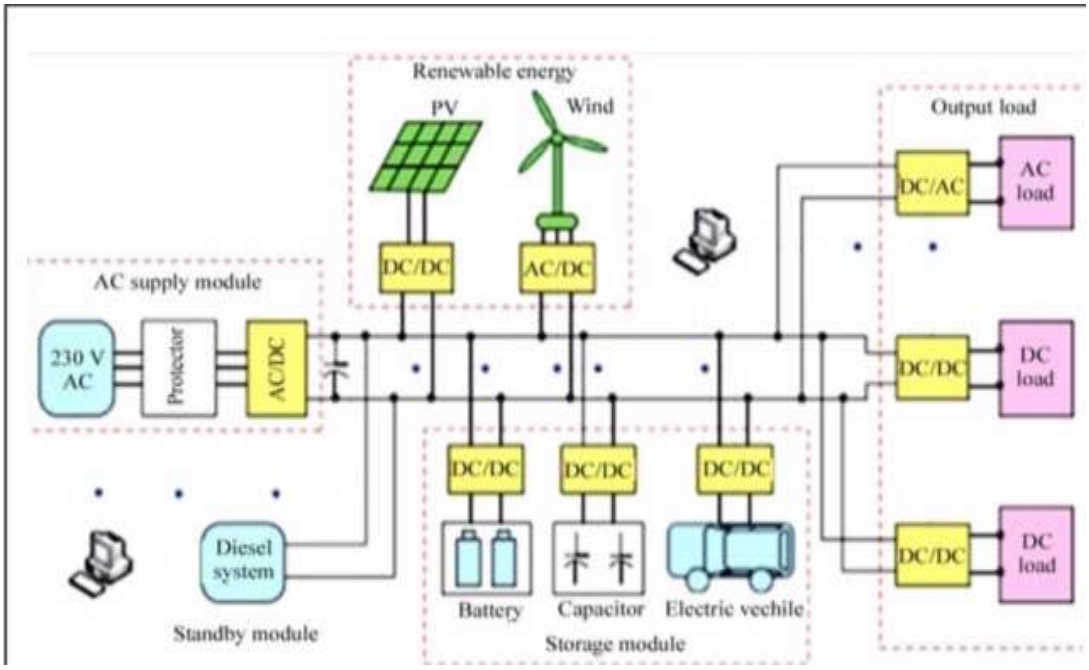

Figure 3.4.- DC Microgrid System

Number of distributed new Energy Resources are Direct Current (DC), for example photovoltaic PV Generation , Stationary Batteries, Mobile Batteries and Fuel cell. The figure 2.4 shows DC Micro Grid Lay Out System. The more energy efficiency, increased economic

operation, constant load maintain. It had to be used DC bus in Micro Grid system its remove number of converting equipment's when compared to AC system. DC Micro Grid Advantages are in given below:

1. To reduce the energy dissipation

2. The Distributed Photovoltaic units is to be increased

3. The Black out of the Commercial Grids, when power supply flow from required load through daily worked distribution lines.

3.4 AC Micro Grid:

The AC Bus system is to be connected all DER's and loads in the AC Micro Grid operation. We observed that circuit diagram as shown in figure 2.5. The energy storing DC generating units have connected to the AC By Via DC to AC Inverters a Rectifying operation is convert to AC to DC the power supplying to the DC loads.

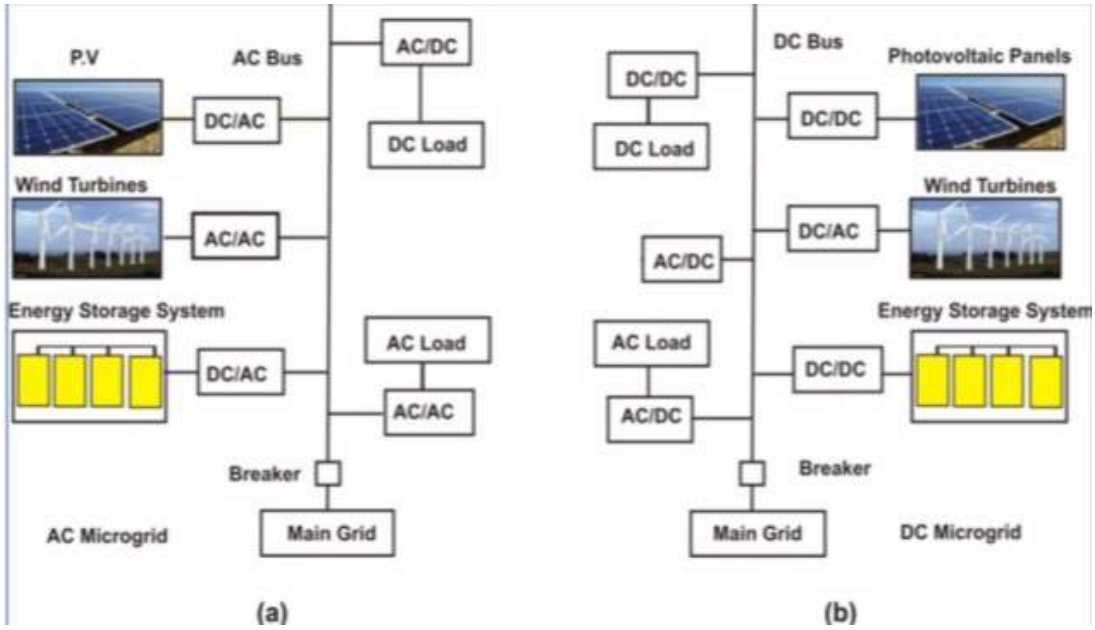

Figure 3.5 (a) AC Microgrid (b) DC Microgrid

3.5 AC/ DC Microgrid:

This idea gives a new pattern for the meaning of the distributed generation operation. To the utility purpose the microgrid can be considered as a controlled cell of the power system. To the user the microgrid can be planned to their find special requirements where , improvement

of community reliability, removing of feeder losses, community voltages support, expand efficiency via waste heat revival scheme, voltage sag adjustment. The microgrid or distribution structure before system had generate less concern to the used system than the conventional micro generation if there is accurate and creative arrangement of micro generation and loads. This hybrid model can be seen through figure 236 below

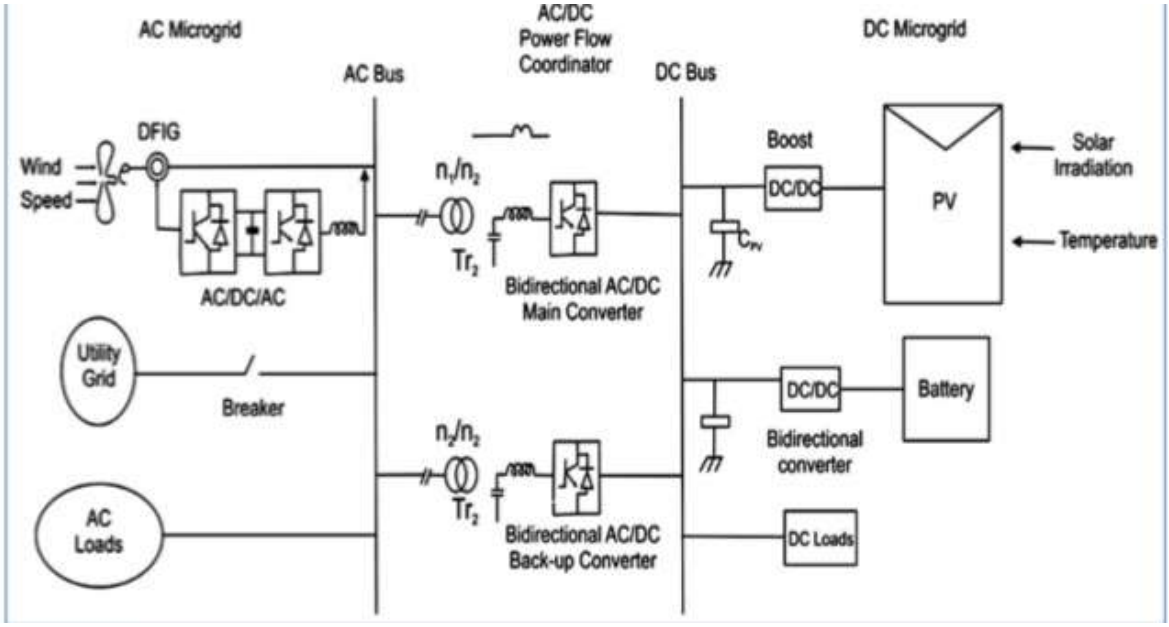

Figure 3.6- Hybrid AC/DC Microgrid System

From the above figure we can say there are various AC and DC sources and loads which connected to the corresponding AC and DC networks. The AC and DC links are linked simultaneous during two transformers and two four quadrants running three phase converters. The AC bus of the hybrid grid is fixed to the point grid.

3.6 Importance of Micro grid

Micro grids provide the most promising means of integrating large amounts of distributed resources into the power grid. Peculiarity, it is great for conventional energy resources to better sustainability, since a developing number of organizations and government's location a higher expense on renewable energy generation .

The broad entrance of renewable also decrease emissions. The U.S. Department of Defence (DOD) has identification reliability on the use grid as an important vulnerability to their mission because of developing threats to power control and using systems. A micro grid can provide higher reliability against such a threat. Hospitals, Universities, Refineries, pharmaceutical manufacturing company, online centres and research laboratories have a strategic necessity for constant power and cannot affray blackouts.

Today, these organizations have backup generators for emergencies. A micro grid can better utilize these backup generators with automated controls in a micro grid and provide a reliable power system. In addition, they offer energy security and surety to critical loads. Further, they open the door to important system efficiency improvements used Combined Heating and Power (CHP).Unlike electricity, Heat is used the form of steam or hot water and cannot be easily or econometric transported a longest distance. CHP indicates a collective energy system that given both electricity and useful heat from an energy source such as natural gas. Micro grids can also provide additional benefits to the local utility by providing dispatch able power for use during peak power conditions. They generate opportunity for electricity market players in terms of additional services. User and businesses can give beneficial services plus demand reaction, real time price return, and voltage support to the grid in response for payments from the serving utilize or self-contained system operator.

CHAPTER-4

AC-DC CONVERTER

4.1 Introduction

Single phase uncontrolled d rectifiers are extensively used in a number of power electronic based converters. In most cases they are used to provide an intermediate unregulated dc voltage source which h is further processed to obtain a regulated dc or ac output. They have, in general, been proved to be efficient and robust power stages. However, they suffer from a few disadvantages. The main among them is their inability to control the output dc voltage / current magnitude when the input ac voltage and load parameters remain fixed. They are also unidirectional in the sense that they allow electrical power to flow from the ac side to the dc side only. These two disadvantages are the direct consequences of using power diodes in these converters which can block voltage only in one direction. As will be shown in this module, these two disadvantages are overcome if the diodes are replaced by thyristors, the resulting converters are called fully controlled converters.

Thyristors are semi controlled devices which can be turned ON by applying a current pulse at its gate terminal at a desired instance. However, they cannot be turned off from the gate terminals. Therefore, the fully controlled converter continues to exhibit load dependent output voltage / current waveforms as in the case of their uncontrolled counterpart. However, since the thyristor can block forward voltage, the output voltage / current magnitude can be controlled by controlling the turn on instants of the thyristors. Working principle of thyristors based single phase fully controlled converters will be explained first in the case of a single thyristor half wave rectifier circuit supplying an R or R-L load. However, such converters are rarely used in practice. Full bridge is the most popular configuration used with single phase fully controlled rectifiers. Analysis and performance of this rectifier supplying an R-L-E load.

4.2 Single Phase Fully Controlled Half Wave Rectifier

Resistive load:

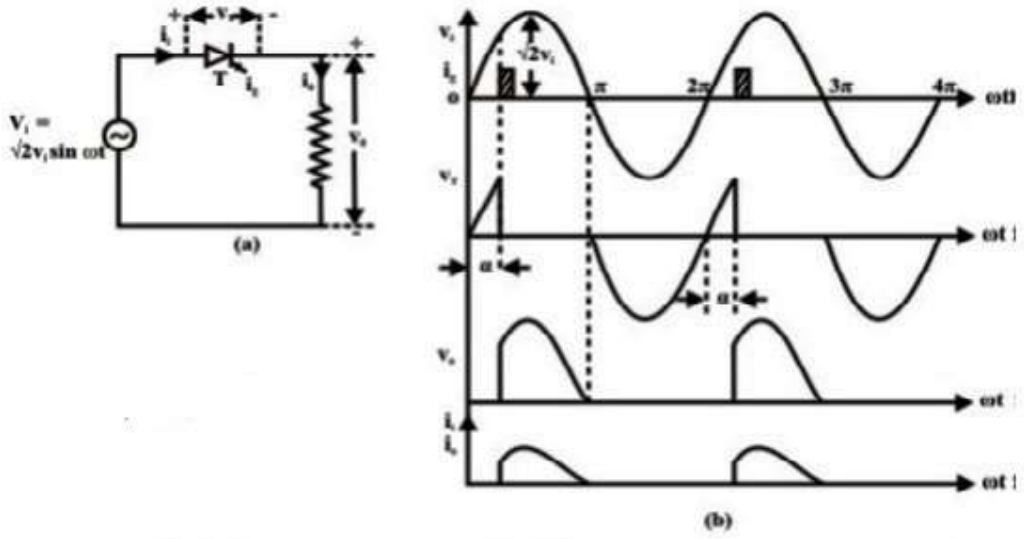

Fig.4. 1(a) single phase fully controlled half wave rectifier supplying a purely resistive load and (b) Wave forms.

Fig.4. 1(a) shows the circuit diagram of a single phase fully controlled halfwave rectifier supplying a purely resistive load. At ωt = 0 when the input supply voltage becomes positive the thyristor T becomes forward biased. However, unlike a diode, it does not turn ON till a gate pulse is applied at ωt = α. During the period 0 <ωt ≤ α, the thyristor blocks the supply voltage and the load voltage remains zero as shown in fig 3.1(b). Consequently, no load current flows during this interval. As soon as a gate pulse is applied to the thyristor at ωt = α it turns ON. The voltage across the thyristor collapses to almost zero and the full supply voltage appears across the load. From this point onwards the load voltage follows the supply voltage. The load being purely resistive the load current i_o is proportional to the load voltage. At ωt = π as the supply voltage passes through the negative going zero crossing the load voltage and hence the load current becomes zero and tries to reverse direction. In the process the thyristor undergoes reverse recovery and starts blocking the negative supply voltage. Therefore, the load voltage and the load current remain clamped at zero till the thyristor is fired again at ωt = 2π + α. The same process repeats thereafter.

From the discussion above and Fig 2.1 (b) one can write

For α<ωt≤π

$V_0 = V_i = \sqrt{2} V_i \sin\omega t$ ……(4.1)

$I_0 = \frac{V_o}{R} = = \sqrt{2}\frac{V_i}{R}\sin\omega t$ ……(4.2)

$V_0 = i_0 = 0$ otherwise

Therefore $V_{0AV} = \frac{1}{2\pi}\int_0^{2\pi} V_o \, d\omega t = \frac{1}{2\pi}\int_0^{\pi}\sqrt{2}\, V_i \sin\omega t \, d\omega t$ ……(4.3)

Or $V_{0AV} = \frac{V_i}{\sqrt{2}\pi}(1+\cos\alpha)$ ……(4.4)

$V_{0RMS} = \sqrt{\frac{1}{2\pi}\int_0^{2\pi} V_o^2 d\omega t}$ ……(4.5)

$\therefore FF_{V0} = \frac{V_o rms}{V_o AV} = \frac{\pi(1-\frac{\alpha}{\pi}+\frac{\sqrt{\sin 2\alpha}}{2\pi})}{(1+\cos\alpha)}$ ……(4.6)

Similar calculation can be done for i_0. In particulars for pure resistive loads $FF_{io} = FF_{vo}$.

Resistive-Inductive load

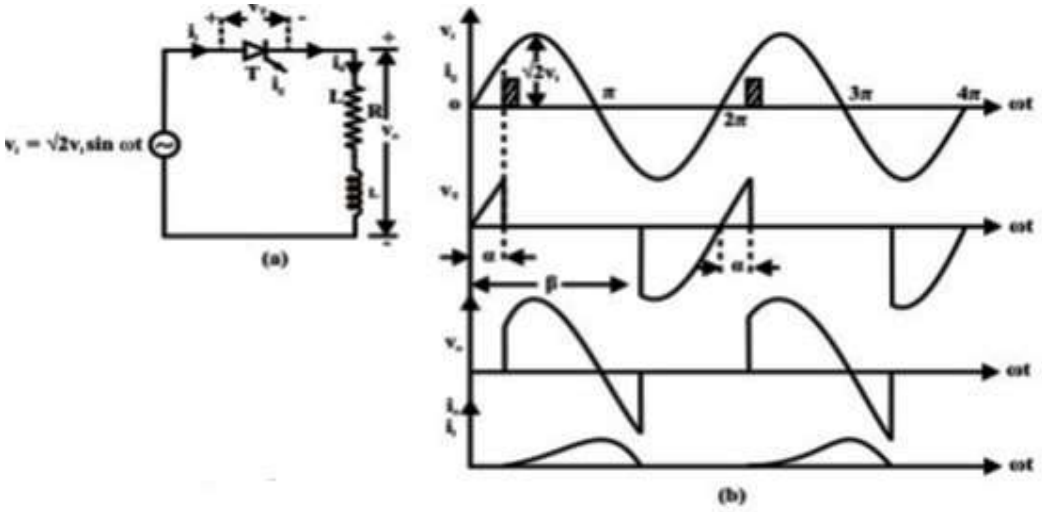

Fig 4.2(a) single phase fully controlled half wave rectifier supplying a resistive inductive load and (b)waveforms.

Fig 4.2 (a) and (b) shows the circuit diagram and the waveforms of a single phase fully controlled half wave rectifier supplying a resistive inductive load. Although this circuit is hardly used in practice its analysis does provide useful insight into the operation of fully controlled rectifiers which will help to appreciate the operation of single-phase bridge converters to be discussed later.

As in the case of a resistive load, the thyristor T becomes forward biased when the supply voltage becomes positive at ωt = 0. However, it does not start conduction until a gate

pulse is applied at ωt = α. As the thyristor turns ON at ωt = α the input voltage appears across the load and the load current starts building up. However, unlike a resistive load, the load current does not become zero at ωt = π, instead it continues to flow through the thyristor and the negative supply voltage appears across the load forcing the load current to decrease. Finally, at ωt = β (β > π) the load current becomes zero and the thyristor undergoes reverse recovery. From this point onwards the thyristor starts blocking the supply voltage and the load voltage remains zero until the thyristor is turned ON again in the next cycle. It is to be noted that the value of β depends on the load parameters. Therefore, unlike the resistive load the average and RMS output voltage depends on the load parameters. Since the thyristors does not conduct over the entire input supply cycle this mode of operation is called the "discontinuous conduction mode".

From above discussion one can write.

$$For\ \alpha \le \omega t \le \beta$$

$$V_o = V_i = \sqrt{2}V_i sin\omega t \qquad \ldots\ldots\ldots\ldots\ldots\ldots\ldots\ldots\ldots\ldots\ldots\ldots\ldots\ldots\ldots.(4.7)$$

V_o=0 otherwise

$$V_{OAV} = \frac{1}{2\pi}\int_0^{2\pi} V_o sin\omega t \ldots\ldots\ldots\ldots\ldots\ldots\ldots\ldots\ldots\ldots\ldots\ldots\ldots\ldots\ldots\ldots\ldots\ldots\ldots\ldots\ldots.(4.8)$$

$$= \frac{1}{2\pi}\int_\alpha^\beta \sqrt{2}V_i sin\omega t\ d\omega t$$

$$= \frac{V_i}{\sqrt{2}\pi}(cos\alpha - cos\beta)$$

$$V_{ORMS} = \sqrt{\frac{1}{2\pi}\int_0^{2\pi} v_0^2\ d\omega t}$$

$$= \sqrt{\frac{1}{2\pi}\int_\alpha^\beta 2v_i^2 sin^2\omega t\ d\omega t}$$

$$= \frac{V_i}{\sqrt{2}}\left(\frac{\beta-\alpha}{\pi} + \frac{sin2\alpha - sin2\beta}{2\pi}\right)^{\frac{1}{2}} \ldots\ldots\ldots\ldots\ldots\ldots\ldots\ldots\ldots\ldots\ldots\ldots.(4.9)$$

$$I_{OAV} = \frac{V_{OAV}}{R} = \frac{V_i}{\sqrt{2}\pi R}(cos\alpha - cos\beta)\ldots\ldots\ldots\ldots\ldots\ldots\ldots\ldots\ldots\ldots\ldots(4.10)$$

Since the average voltage drop across the inductor is zero.

However, I_{ORMS} cannot be obtained from V_{ORMS} directly. For that a closed from expression for i_0 will be required. The value of β in terms of the circuit parameters can also be found from the expression of i_0.

$$For\ \alpha \leq\ \omega t \leq\ \beta$$

$$L\frac{di_o}{dt} + R\, i_o + E = \sqrt{2}V_i sin\omega t \ldots\ldots\ldots\ldots\ldots\ldots\ldots\ldots\ldots\ldots\ldots\ldots (4.11)$$

The general solution of which is given by

$$i_0 = I_0 e^{-\frac{(\omega t-\alpha)}{tan\phi}} + \frac{\sqrt{2}V_i}{Z} sin\,(\omega t - \phi) \ldots\ldots\ldots\ldots\ldots\ldots\ldots\ldots\ldots\ldots\ldots\ldots\ldots\ldots (4.12)$$

$$Where\ \ tan\phi = \frac{\omega L}{R}\ and\ Z = \sqrt{R^2 + \omega^2 L^2}$$

$$i_{0\,|\,\omega t=\alpha} = 0$$

$$0 = I_0 = \frac{\sqrt{2}V_i}{Z} sin\,(\alpha - \beta)$$

$$i_0 = \frac{\sqrt{2}V_i}{Z}\left[sin(\alpha - \beta)\, e^{-\frac{(\omega t-\alpha)}{tan\phi}} + sin\,(\omega t - \phi)\right] \ldots\ldots\ldots\ldots\ldots\ldots\ldots\ldots\ldots\ldots (4.13)$$

$I_0=0$ otherwise

Equation (4.13) can be used to find out I_{ORMS}. To find out β it is noted that

$i_o|_{\omega t=\beta} = 0$

$$\therefore sin(\varphi - \alpha)\, e^{\frac{\alpha-\beta}{tan\varphi}} = sin(\varphi - \beta) \ldots\ldots\ldots\ldots\ldots\ldots\ldots\ldots\ldots\ldots\ldots\ldots (4.14)s$$

4.3 Single Phase Fully Controlled Bridge Converter

Fig 4.3 (a) shows the circuit diagram of a single phase fully controlled bridge converter. It is one of the most popular converter circuits and is widely used in the speed control of separately excited dc machines. Indeed, the R–L–E load shown in this figure may represent the electrical equivalent circuit of a separately excited dc motor.

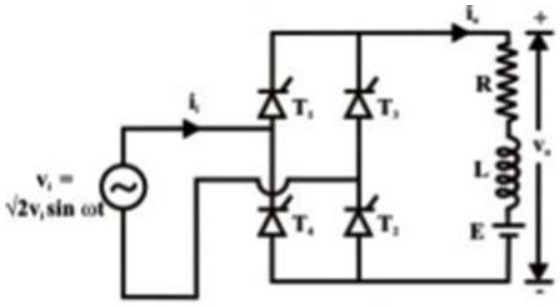

MODE / DEVICE	T_1	T_2	T_4	T_3	v_o
T_1T_2	0	0	$-v_i$	$-v_i$	v_i
T_3T_4	v_i	v_i	0	0	$-v_i$
NONE	$\frac{v_i - E}{2}$	$\frac{v_i + E}{2}$	$-\frac{v_i + E}{2}$	$-\frac{v_i + E}{2}$	E

Fig 4.3 Single phase fully controlled bridge converter. Table 4.1 Conduction table.

The single phase fully controlled bridge converter is obtained by replacing all the diode of the corresponding uncontrolled converter by thyristors. Thyristors T_1 and T_2 are fired together while T_3 and T_4 are fired 180º after T_1 and T_2. From the circuit diagram of Fig 2.1 (a) it is clear that for any load current to flow at least one thyristor from the top group (T_1, T_3) and one thyristor from the bottom group (T_2, T_4) must conduct. It can also be argued that neither T_1T_3 nor T_2T_4 can conduct simultaneously. For example, whenever T_3 and T_4 are in the forward blocking state and a gate pulse is applied to them, they turn ON and at the same time a negative voltage is applied across T_1 and T_2 commutating them immediately. Similar argument holds for T_1 and T_2.

For the same reason T_1T_4 or T_2T_3 cannot conduct simultaneously. Therefore, the only possible conduction modes when the current i_0 can flow are T_1T_2 and T_3T_4. Of course, it is possible that at a given moment none of the thyristors conduct. This situation will typically occur when the load current becomes zero in between the firings of T_1T_2

and T_3T_4. Once the load current becomes zero all thyristors remain off. In this mode the load current remains zero. Consequently, the converter is said to be operating in the discontinuous conduction mode. Fig 4.3(b) shows the voltage across different devices and the dc output voltage during each of these conduction modes. It is to be noted that whenever T_1 and T_2 conducts, the voltage across T_3 and T_4 becomes $-v_i$. Therefore, T_3 and T_4 can be fired only when $v_i$is negative i.e, over the negative half cycle of the input supply voltage. Similarly, T_1 and T_2 can be fired only over the positive half cycle of the input supply. The voltage across the devices when none of the thyristor's conduct depends on the off-state impedance of each device. The values listed in Fig 4.3 (b) assume identical devices. Under normal operating condition of the converter the load current may or may not remain zero over some interval of the input voltage cycle. If i_0 is always greater than zero then the converter is said to be operating in the continuous conduction mode. In this mode of operation of the converter T_1T_2 and T_3T_4 conducts for alternate half cycle of the input supply.

However, in the discontinuous conduction mode none of the thyristors conduct over some portion of the input cycle. The load current remains zero during that period.

CHAPTER-5

PROPOSED TOPOLOGY

5.1 Control Strategies:

The considered DC micro grid includes a non- dispatchable generator (solar-PV) and dispatchable generators (micro turbine, fuel-cell) and loads, as shown in Fig. 1. The non-dispatchable-solar PV system is set to operate in current control mode and thus extracts maximum power at all the times. The dispatchable generators are typically used for firming the renewable capacity and can be controlled either through a centralized or decentralized control scheme. The decentralized droop scheme is the most widely used and preferred, as it is simple and reliable. Therefore, the traditional droop (P-V)scheme has been used for the dispatchable generators of the DC micro grid (see Fig. 1), which is given by

$$V_{dc,ref,i} = V_{dc,max} - \partial_{dc,i} P_{dc,i}$$

$$\partial_{dc,i} = \frac{V_{dc,max} - V_{dc,min}}{P_{dc,max,i}} = \frac{\Delta V_{dc}}{P_{dc,max,i}} \qquad (1)$$

where, i is the DC generator number (i = 1, 2, 3. . .); Vdc,ref,$I$is the reference voltage of ith generator; Pdc ,$i$is the output power of ith generator; Vdc, max and (V dc,min= Vdc,nom,TC1) are the defined maximum and minimum voltage; Pdc, max,I is the maximum or rated power of ith generator; and ∂dc ,I is the droop gain of ith generator. Based on (1), the voltage reference for the droop-controlled generators 1 and 2 can be calculated by (2) and (3).As generators 1 and 2 share common DC bus voltage (i.e.,Vdc,ref,1 = Vdc,ref,2), (2) and (3) can be equated and rewritten by (4), which demonstrates that the droop-controlled generator will share proportional power according to their rated power capacity.

$$V_{dc,ref,1} = V_{dc,max} - \partial_{dc,1} P_{dc,1} \quad (2)$$

$$V_{dc,ref,2} = V_{dc,max} - \partial_{dc,2} P_{dc,2} \quad (3)$$

$$\partial_{dc,1} P_{dc,1} = \partial_{dc,2} P_{dc,2} \rightarrow \frac{P_{dc,1}}{P_{dc,max,1}} = \frac{P_{dc,2}}{P_{dc,max,2}} = \frac{P_{dc,i}}{P_{dc,max,i}} \quad (4)$$

The generator terminals are the same. Practically, the voltage at all the generator terminals is not the same due to the fact that they are connected through feeders/cables of different lengths. This voltage mismatch at the generator terminals affects the power sharing accuracy, which needs to be compensated by using any of the appropriate compensation

methods. The droop equation with compensation of the feeder voltage drop can be rewritten by

$$V_{dc,ref,i} = v_{dc,max} - \partial_{dc,i} P_{dc,i} + I_{dc,i} X_i \quad (5)$$

The voltage of the droop-controlled DC microgrid will vary with the changing load, but within the defined permissible range. For the considered DC microgrid, the voltage range with increased aggregated loading is shown in Fig. 1 (bottom left). For the droop-controlled generators, the voltage range I set between 395 V and 420 V, indicating that the generators will deliver no-power at 420 V and 100% power at 395 V. Once the DC generators are heavily loaded (e.g., $\leq$ 402.5 V at80% generators loading), the tie-converters will start to import power from the AC micro grid to meet the peak load demand, and also regulate the voltage of the DC micro grid.

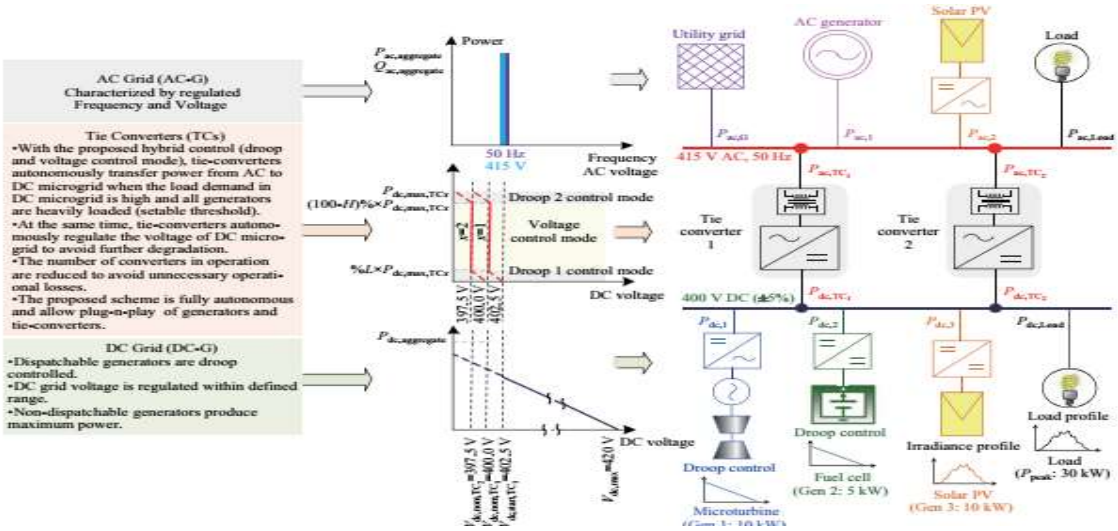

Fig. 5.1. Interlinked AC-DC microgrids and their control strategy.

For the example of interlinked micro grids in Fig. 1, the voltage and frequency of the AC micro grid is considered stiff. The AC micro grid can be droop controlled with secondary voltage and frequency regulation, or operating in grid-connected mode. The characteristics of the AC micro grid are shown in Fig. 1,where the voltage and frequency are constant at nominal value (e.g., 50 Hz and 415 V). In addition, the AC micro grid has sufficient generation capacity to meet its local demand and export surplus power to the DC micro grid which has been demonstrated through the proposed autonomous control of the tie-converters. The details of the tie-converters control are given in Section III.

5.2. Proposed Hybrid Control Of Tie-Converters

The power rating of dispatchable generators or storage systems for firming the renewable capacity depends on the variability of the renewable source and loads in the microgrid. The high variability of renewables and loads requires dispatchable generators or storage systems with a high-power rating, which may or may not be a viable solution. Alternatively, the microgrid with inadequate generation capacity could be interconnected with another microgrid or utility grid, directly or through harmonizing converters. The tying of a DC microgrid with an AC microgrid or utility grid is only possible through tie-converters, as shown in Fig. 1. In the proposed interlinked system, the AC microgrid is characterized as a regulated voltage and frequency system with adequate generation capacity, whereas the DC microgrid is characterized as a droop-controlled system with inadequate generation capacity due to the high variability of the renewable and loads. During the peak demand or the low renewable power output, the power deficit in the DC microgrid is managed by importing power from the AC microgrid. Ideally, it can be achieved efficiently and autonomously with the proposed control of the tie-converters. In summary, the control scheme of the tie-converters is developed based on the following objectives: 1) To transfer power from the AC to DC microgrid during the peak load demand or generation contingency in the DC microgrid; 2) To minimize the power transfer losses, e.g., tie-converter should operate only during the peak-load demand in the DC microgrid, and the number of tie-converters in operation should be based on power transfer demand; 3) To regulate the voltage of the droop controlled DC microgrid; 4) To achieve fully autonomous control without depending on the communication network; 5) To enable the plug-n-play feature for tie-converters and generators. Unlike the existing schemes for the interlinked AC-DC microgrids [18]–[22], a hybrid droop and voltage regulation mode control are proposed for the tie-converters and the mathematical form of the proposed control scheme is given by

$$V_{dc,ref,TCx} = \begin{cases} Off; \\ V_{dc,start,TCx} - \delta_{L,TCx} \times P_{dc,TCx}; \\ V_{dc,nom,TCx}; \\ V_{dc,nom,TCx} - \delta_{H,TCx}[P_{dc,TCx} - (100-H)\% \times P_{dc,max,TCx}]; \end{cases}$$

where TCx represents the tie-converter number (x = 1, 2, 3..);Vdc is the DC microgrid voltage; Vdc,ref,TC$x$is the reference voltage of xth tie-converter; Vdc,start,TC$x$is the threshold voltage to start of xth tie-converter; Vdc,nom,TC$x$is the nominal voltage to be regulated by xth tie-converter; Pdc,TC$x$is the DC power output of xth tie-converter;

*P*dc,max,TC*x* is the maximum power limit of *x*th tie-converter; *L*% and *H*% are the percentage of tie-converter rated power allocated for droop1 and 2 mode, respectively; Vdc,nom,TCx+1 is the DC microgrid voltage when xth tie-converter transfers maximum power; δL,TCx= (Vdc,start,TCx - Vdc,nom,TCx)/(L% ×Pdc,max,TCx) is the droop 1 gain (at low power) of xth tie converter; δH,TCx= (Vdc,nom,TCx - Vdc,nom,TCx+1)/(H% ×Pdc,max,TCx) is the droop 2 gain (at high power) of xth tie converter. As shown in Fig. 1, tie-converter 1 starts in droop 1 control mode when the voltage in the DC microgrid drops to the set threshold of Vdc,start,TCx. This voltage threshold implies that all the generators in the DC microgrid are heavily-loaded (e.g., over 80% loaded). The start of the tie-converter in the droop control mode enables a smooth transition to the voltage regulation mode at the set condition i.e., Pdc,TCx> L% × Pdc,max,TCx. During the voltage regulation mode, the tie-converter imports power from the AC microgrid to meet the DC microgrid peak power demand as well as regulate its voltage to be set to the nominal value of Vdc,nom,TCx. Furthermore, unlike the parallel operation of all tie converters in the existing schemes, the converters operation has been prioritized. The first tie-converter only starts when all the generators in the DC microgrid are heavily-loaded. Once the first tie-converter power capacity is near to saturation at Pdc,TCx= (100 - H)% × Pdc,max,TCx, its control mode is changed from the voltage regulation to droop 2 control mode to allow minor voltage drop. This minor voltage drop caused by the droop 2 control mode will enable the next tie-converter to start its operation. In case of failure of the first tie-converter, the second tie-converter will automatically start its operation followed by the voltage drop due to high load demand. Therefore, the proposed control strategy ensures efficient operation during all operating conditions without compromising the inherited flexibility of the droop-based scheme. The allocation of the tie-converter's power for droop1 and droop 2 control mode depends on the chosen value of L% and H% which are user definable, and should be tuned to allow smooth transition between different modes while considering the voltage and power measurement tolerance/errors in the considered microgrid. With the proposed voltage regulation mode, the overall voltage regulation performance of the DC microgrid can be improved. In particular during the peak load demand, the

$$V_{dc} > V_{dc,start,TCx}$$

$$0 \le P_{dc,TCx} \le L\% \times P_{dc,max,TCx}$$

$$L\% \times P_{dc,max,TCx} < P_{dc,TCx} < (100-H)\% \times P_{dc,max,TCx}$$

$$(100-H)\% \times P_{dc,max,TCx} \le P_{dc,TCx} \le P_{dc,max,TCx}$$

voltage of the DC micro grid is regulated at the nominal value, which is not the case with the existing power management schemes for interlinked micro grids. The performance of the proposed scheme has been validated for different load operating scenarios, as described in Section 5.3

5.3. Performance Validation

The performance of the proposed scheme has been validated for two different scenarios of the DC microgrid. In the first scenario, the microgrid comprises dispatchable microturbine (Gen 1), fuel cell (Gen 2) and variable load. In the second scenario, a non-dispatchable solar PV generator (Gen 3) is Added to scenario 1. The system parameters are summarized in Tables I–III.TABLE I

CONTROL MODE OF DC AND AC MICROGRIDS

Entity	Control Mode	
AC microgrid	Islanded-microgrid with regulated voltage and frequency Grid-connected mode	
Tie-converter	Hybrid droop and voltage control mode	
DC microgrid	Dispatchable generators	Droop controlled
	Non-dispatchable generators	Current control mode with MPPT

Description	Parameter	Value
Voltage	V_{dc} (V)	400 (+5%, −1.25%)
Micro-turbine	$P_{dc,max,1}$ (kW)	10
	$\partial_{dc,1}$ (V/kW)	2.5
Fuel cell	$P_{dc,max,2}$ (kW)	5
	$\partial_{dc,2}$ (V/kW)	5
Solar PV	$P_{dc,max,3}$ (kW)	10
Load	$P_{Load,peak}$ (kW)	25

TABLE III
AC MICROGRID AND TIE CONVERTER PARAMETERS

Description	Parameter	Value
AC microgrid	V_{ac} (V)	415 ($l-l$)
	f (Hz)	50
Tie-converter	P_{dc,max,TC_1} (kW)	10
	$V_{dc,start,TC_1}$ (V)	402.5
	V_{dc,nom,TC_1} (V)	400.0
	V_{dc,nom,TC_2} (V)	397.5
	$L\% = H\%$	10%

The mode transition logic of the tie-converter is given in the logic flow diagram shown in Fig. 2, and the detailed control block diagram of the tie-converter is shown in Fig. 3. Both scenarios have been tested at different load operating conditions to demonstrate the robustness and effectiveness of the proposed scheme.

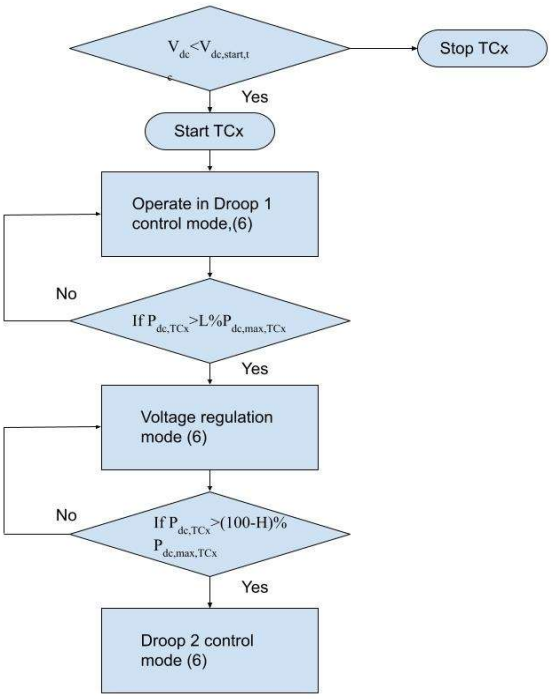

Fig.5. 3 Logic flow diagram showing mode transitions of tie-converter

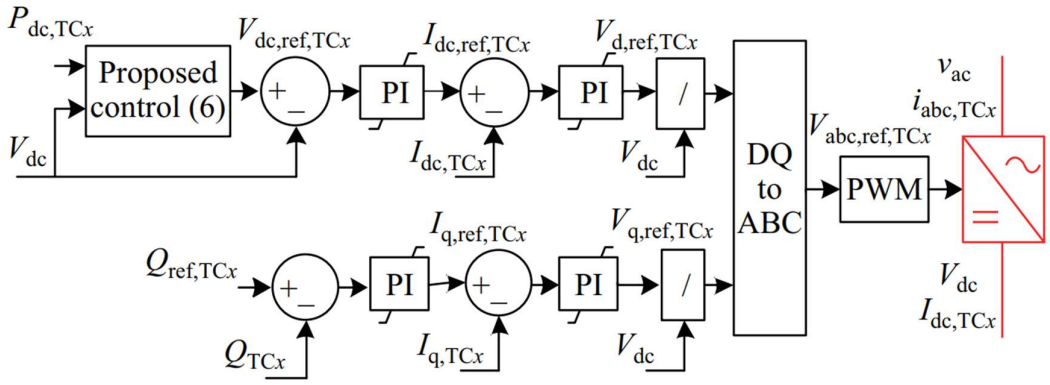

Fig. 5.4. Control block diagram of tie-converter.

CHAPTER-6
CONTROLLERS AND PWM TECHNIQUES

6.1 Introduction

A controller is indeed a tool that has numerous functions that correct the variance generated in comparison with the required regulated variable

The following are the essential implementations of controllers:

• Controllers boost the system to a constant degree of accuracy by reducing the loss in a constant state.

• As a constant condition to enhance accuracy and reliability.

• Removal of offsets would help to increase the device goods.

• For controls utilizing controllers, maximum under-shoot of both the system is needed.

• The noise power given in a device often tends to lower.

• The sluggish over damped device reaction has to be improved more quickly by growing the controller 's performance.

Different controller styles exist. In a device there are 3 kinds:

- P-controller.(Proportional type)
- I-controller. (Integral type)
- D-controller.(Derivative type)

For functional structures, the mixture of PI with PD is most commonly used.

6.2 Proportional- Controller

Such form of controller could not regulate a more proportional operation. We grasp energy conservation for the first time with rising tolerance. Maintaining equilibrium at first order chaotic phase may be proportional controls. Controller modifications benefit K shifts in the structure of the closed loop. That control device improves by a big processor.

• Smaller reliability failures with a clearer comparison at various device positions are increased.

• Quick dynamics include changes throughout the closed loop device signal frequency range, as well as a rise in sensitivity related to noise measurements.

• Lower amplitude but margin of motion.

The output was immediately proportional to the error signals in such a proportional controller.

$$A(t) \alpha e(t) \quad \ldots\ldots \quad 6.1$$

We can compose the equation by eliminating the symbol of proportionality

$$A(t)=K_p * e(t) \quad \ldots\ldots. \quad 6.2$$

Where's the K p named the controller benefit a proportional continuous?

It has suggested which K p be retained beyond unity. When the K p value is higher than unity, another error signal would be shown and the mistake will be quickly identified to further decrease the increased error.

Advantages of Proportional Controller

That proportional controller tends to reduce the error by keeping the steady state through increasing the reliability of a device. Slow response from the given load which rendered the controller that controls the managed appropriately.

Disadvantages of Proportional Controller

Because such controls are present, some configurations are necessary for device offsets.

Proportional controllers can maximize that circuit system's potential leakage.

6.3 Integral-Controller

The unit output operates immediately through an error function equal to both the integral. Now that it is necessary to calculate through writing the formula in the study at such a control system.

$$A(t)\alpha\int_0^t e(t)dt \qquad \ldots\ldots\ldots 6.3$$

Disable the proportionality symbol

$$A(t)=K_i*\int_0^t e(t)dt \qquad \ldots\ldots\ldots 6.4$$

Where was the K i sometimes regarded as the controller obtain an integral continuous? Often known called reset computer, the smart system.

Advantages of Integral Controller

Regardless of their special theories, they have the opportunity to replay the element precisely at a certain stage on a table. Any of the difficulty that makes restore controls.

Disadvantages of Integral Controllers

In addition to slowing down the operation, this would render the device unreliable and trigger a mistake.

6.4 Derivative Controller

The computer could not be equipped for such controls on its own. The models must be regulated by a special program. The derivative drivers with this were at the performance often boost the relation with the derivatives directly related at such an error function. When derivative controller's production, mathematically that error signal function is directly related. It is in the shape of

$$A(t)\alpha\frac{de(t)}{dt} \qquad \ldots\ldots 6.5$$

Removing the sign of proportionality, we have

$$A(t)=K_d*\frac{de(t)}{dt} \qquad \ldots\ldots 6.6$$

Where was the K_d sometimes regarded as the system benefit proportional constant? Often named a levels processor is the differential processor.

Advantages of Derivative Controller

The key benefits of the differential controller improve a system's transient reaction.

Disadvantages of Derivative Controller

Without any of the transmitter, it never increases the stationary malfunction.

This induces symptoms of distortion and thus amplifies that system's noise.

6.5 Proportional And Integral Controller

This mixture of conditional and integrated controls becomes part of both the instrument that enhances outcomes. This method, which is also known as an acting signal, is the amount of proportional and integral to support the signal locate. Using mathematically to determine the directly equivalent, by way of error summarization and signal analysis,
We will compose as follows

$$A(t)\alpha \int_0^t e(t)dt + A(t)\ \alpha\ e(t) \qquad \ldots\ldots\ 6.7$$

Removing the sign of proportionality we have,

$$A(t) = kd \int_0^t e(t)dt + A(t) + kpe(t) \qquad \ldots\ldots\ 6.8$$

In attempt to discover the effects of the activity to switch in and out of the system, PI controller must eliminate force oscillatory and settling time error. That being said, an interconnected paradigm may be implemented that influences a system 's undesirable shape and general reliability.

That PI controller does therefore not improve the speed performance and overall device stability. Also, because PI controller is not anticipating whether the device fault is regulated, the issue can be overcome easily and the response period is decreased in a device at the processor. PI controller will improve industry operations, throughout particular to improve the pace and device reaction. A D mode regulation that's also required for the operation to be increased.

a) The system's quick response isn't really sufficient

b) Throughout the activity of the cycle there are significant disruptions and noise

C) just one energy storage (inductive and capacitive) is required in the cycle

d) The network is prone to major transport delays

The PI controller was described as arithmetically

$$A(t)\ \alpha \int_0^t e\ (t)dt + A(t)\ \alpha\ e(t) \qquad \ldots\ldots\ 6.9$$

Removing the sign of proportionality, we have,

$$A(t)\ \alpha\ K_{id}\int_0^t e\ (t)dt + Kpe(t) \qquad \ldots\ldots\ 6.10$$

Parameter	Rise time	Overshoot	Settling Time	S.S error	Stability
K_p	Decrease	Increase	Small Change	Decrease	Worse
K_i	Decrease	Increase	Increase	Significant Dec	Worse
K_d	increase	increase	increase	No change	Better

Table6.1: Effects of changing parameters

That table above demonstrates the results of varying concentrations with multiple devices.

Logical structures in traditional multivalve.

6.6 Modulation Techniques

Your multi-level inversion method produces sinusoidal tension and is programmed to boost specific voltage levels, creating PWM technique to complete assignments generating sinusoid with variable voltage level. That hybrid multi story inverter which can be used with various voltages and frequencies requires to be developed using modulation methods. Modulation approaches may be used to identify the PWM methods employed by the Hybrid converters multi-level modulating device for achieving a large linear modulation, less switching failure and a decrease in frequency harmonic total distortion (THD).

6.7 Types of Modulation Strategies

The much more widely employed approaches for pulse execution of technique modulation. This is one of the PWM (SPWM) but space vector multi-level substations. The reason which SVPWM takes different methods into consideration there is a need to develop the waves graph. This is an improvement over SPWM which increase performance of dc bus voltage, decreased frequency of switching but low current rips. The foregoing are specific techniques:

1. Carrier-based Pulse-Width Modulation.

2. Selective harmonic elimination.

3. Space vector pulse width modulation.

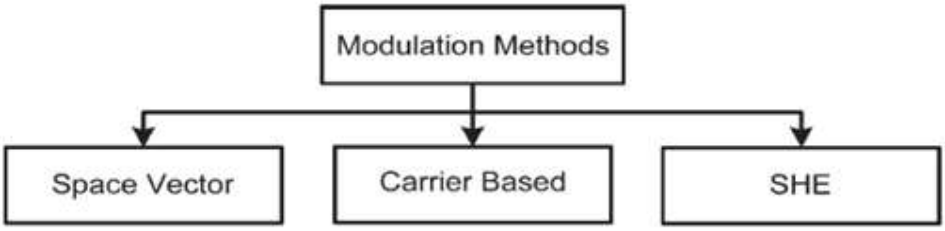

Fig. 6.2: Modulation methods for the three-level diode-clamped inverter

Carrier-Based Three-Level PWM Modulation

It is a very common approach for overcoming the comparative problems. The approaches are quite common since a sinuous comparison with different carriers υcr1 and υcr2 is contrasted. As Fig indicates. 6.3, with basic calculations below the rationale is very conveniently visible,

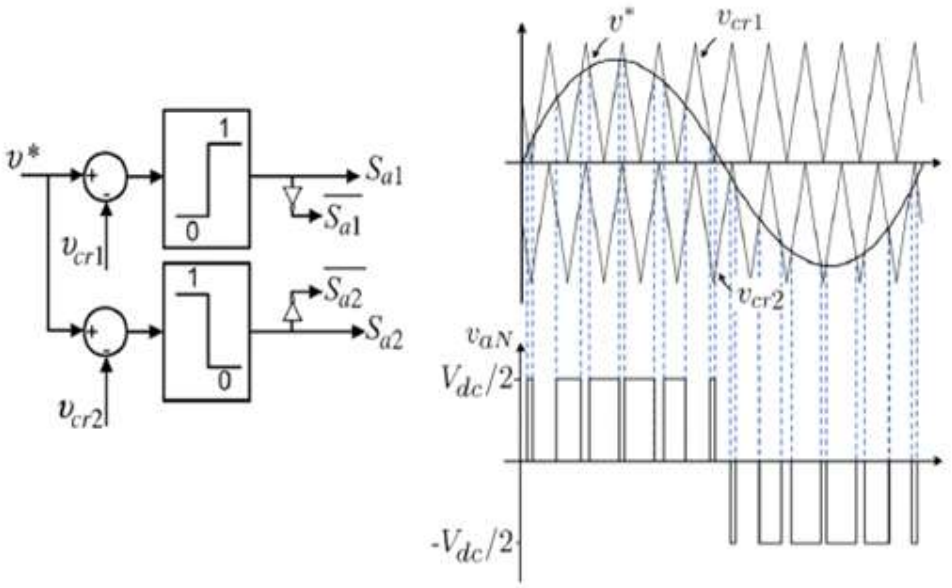

Fig. 6.3: Carrier-based PWM modulator

If $\upsilon^* > \upsilon_{cr1} \Rightarrow S_{a1}=ON \quad S_{a2}=ON \quad \upsilon_{aN}=V_{dc}/2 \quad \ldots\ldots\ldots\ldots 6.11$

$If\ v_{cr2} < v^* < v_{cr1} ==> \overline{Sa1} = ON S_{a2} = ON \qquad v_{aN} = 0 \qquad \ldots\ldots\ldots 6.12$

$If\ v^* < v_{cr21} ==> \overline{Sa2} = ON \qquad v_{aN} = -Vdc/2 \qquad \ldots\ldots\ldots\ldots 6.13$

PWM Carrier Period

With the aid of modulation throughout the inverter lifespan it is possible to monitor the phase with either the PWM input image. The machine frequency & PWM amplitude selection can be enhanced by this approach.

The value is determined according to:

PwmCval = Clk/(2*PwmFreq) 6.14

This same input resolution with U Alpha as well as U Beta signals throughout the Space Vector PWM modulator seems to be 16-bit. The practical resolution of PWM (Pwm,Cval) is therefore constrained either by frequency of the device clock.

Dead Time Insertion Logic

To calculate the performance of each PWM generation machine, that dead period is added. Compared to that same Volt Command Register but boosts the PWM frequency register, such Resolution takes the shape of a 1 clock period or a 30ns at 33,4 MHz clock.

That dead-time induction device trenches Volt second it off of the large side through dead-time but removes the dead-time at such a low side warning. Therefore, the process only at top to activate the pulse would be less than scheduled mostly on dead time throughout commanded volt seconds.

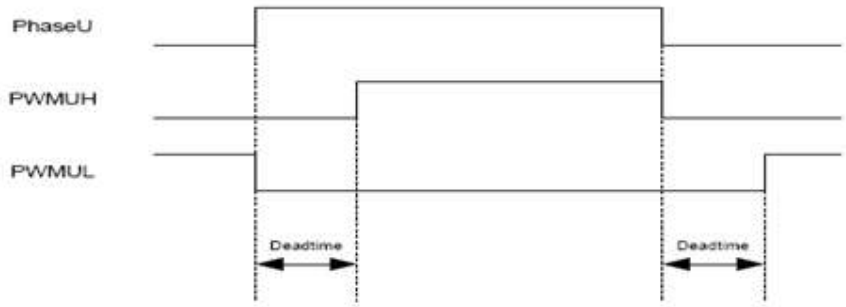

Fig:6.4:Dead time insertion

Deadtime Insertion

That dead time injection indicates the programming period is added between the two top and bottom sides of one step. from the gate signal. This dead-time register also becomes double buffered to allow the machine to adjust during fly dead-time. It allows to regulate the rationale inactively in pulse broad modulation.

CHAPTER-7
MATLAB DESIGN AND SIMULATION RESULTS

7.1 Introduction Of MATLAB:

For scientific programming MATLAB is indeed a high-performance script. That mat research lab name reflects a matrix test. Computing, visualizing, and scripting are combined in a user-friendly setting of questions and answers articulated in common mathematical notation. Mathe and software growth Algorithms Software creation, including interactive user-interface design, including technology research, discovery and visualization. Technology construction Modeling, simulation & prototyping Technology analyzes, explorations and visualizations

MATLAB is indeed a system active engagement, the basic information element of which being array without dimensioning. In a split of period, it will take can develop a code in a scalar, none dynamic language like C or FORTRAN, but you can solve several basic computing problems, of particular those of matrix but Vector Formulizations.

Strengths of MATLAB:

- The learning process of MATLAB is quite simple.
- The programming for MATLAB was designed for just a relatively smooth processing of the matrix.
- TO MATLAB can be calculated or calculated as either a language of programming.
- Towards MATLAB failure can be quickly corrected, represented.
- THE MATLAB has several scientifically driven features, but mainly procedure.

Other features:

Functions enable 2-D and 3-D image visualization.

- Custom programming language interfaces design tools.
- Functions for both the application between externally dependent algorithms, including such C , C++, FORTRAN, Java, Net, and Microsoft office excel.

7.2 SIMULINK:

Just one MATLAB computational eye throughout the Math works seems to be the add-on technology of SIMULINK. A broad numerical processing function powers MATLAB. SIMULINK is indeed a method for the dynamic system (Differential Equations) visually programming and presenting tests. A basic building block throughout SIMULINK libraries may construct any reasoning or control mechanism for just a dynamic device. SIMULINK has many tool boxes that increase the computing ability of both the tool, like Fuzzy Logic, genetic algorithms, DSP, Statistics and so on. The key benefit is that templates / components are usable, such that specific mathematical procedures are not needed to type code.

Concept of signal and logic flow:

SIMULINK transfers data / data from different blocks through lines connecting the respective blocks to some other block. Information may be generated for signals. Then you can dump information into sinks that can be displayed but rather saved to something like a file. Data may be plugged in, inserted etc. from one side to another. Data can be stored and distributed in simulation mostly in irregular intervals because both devices are discrete structures. Therefore, a time step (anything else referred to as an implementation time step) becomes necessary and the fastest dynamics in the simulation system decides the specification of this step.

Sources and sinks:

That source library includes primarily the data that the user normally requires during the software. There have been generally numerous sources mostly in MATLAB library, such as waveform functional parameters which are accordingly implemented by each source. each one of these sources has its own functions, such as pulse generators to produce pulses in certain periods. Both of these helps maintain the data right and provide the customer with the appropriate information, which would be user-friendly.

The drops are points where the signal termination takes place. For some further references the data collected are mostly displayed or may even be stored as a script, mostly several block drains are supplied from which the starting block has been used for beginning the simulation. Everything aims to render the app more user-friendly, while offering the right functionality for the consumer. The blocks accessible throughout the source and sink repositories will be seen in fig.3. To avoid warnings of unconnected signals, unused signals must be stopped.

7.3 Continuous And Discrete Systems:

Both complex processes may be studied either constantly or discreetly. SIMULINK allows for such structures to be represented by means of transition, connection blocks, lag blocks, etc.

Non-linear operators:

The major advantage to use tools like SIMULINK seems to be the ability, without technical resolution, to simulate dynamic functions and produce results. A system with non-linearity like saturation, registration function, restricted slew rates, etc. is quite possible to point at analytical solutions.

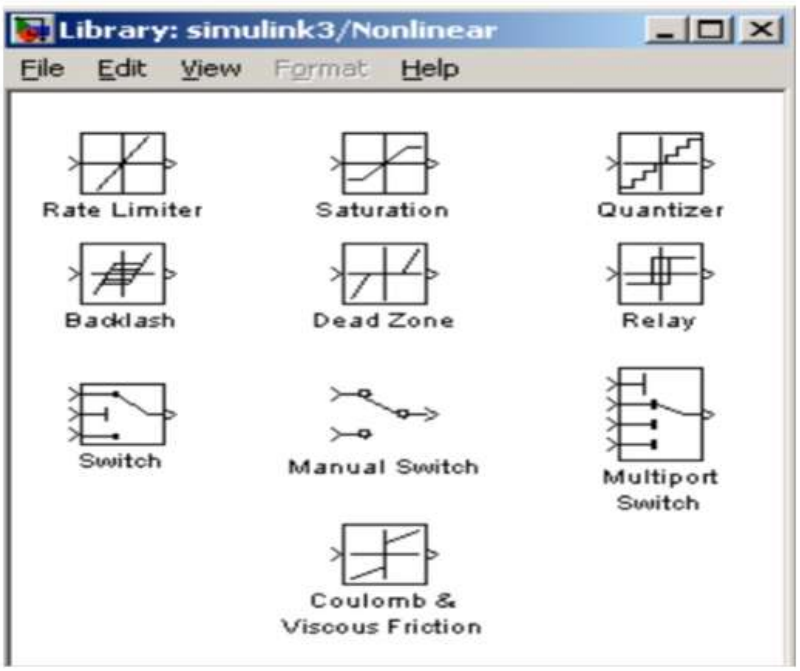

Figure 7.1: SIMULINK blocks

When processes are modeled using loops, in simulation, non-linearity is not an obstacle. The saturation block, for example, may signify a physical parameter restriction, including a voltage signal to either an engine, etc. When testing simulations with various cases, manual circuits are used. Switches are also the functional basis to scripting unless-then statements.

7.4 Mathematical Operations:

That signal flow could be configured along with mathematological users such as items, number, logical operations like and, or, etc. Only with matrix gain unit, matrix multiplication is simple. Also usable are trigonometric functions like sin and tan inversely (at an). In the rational loops, conditional operators, namely 'equal to' or 'larger than' etc.

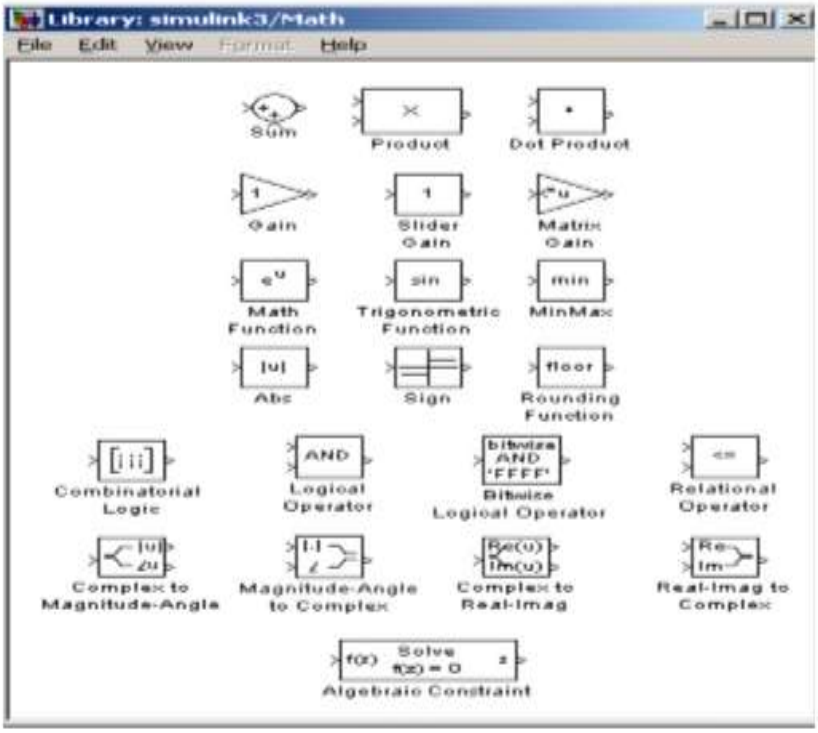

Figure 7.2: SIMULINK math blocks

7.5 Signals And Data Transfer:

Data can be transferred from one section of both the frame to some other part of the frame in dynamic block diagrams. It might be in increasing subsystems. This signal may be deposited into some kind of block that transfers signals between subsystem through subsystem. Multiplexing helps eliminate congestion due to redundant connections and enables the representation of the matrix (column / row). Creating subsystems drags and positions it into the current block wherever you want and to mask the SIMULINK application browser subsystem. The subsystem technique relies mostly on block's function. Typically, the main subsystem is used, though some subsystems are chosen. For e.g., the subsystem may be an active block that only requires any trigger signal. Open another subsystem (double click) but build PORTS for input / output, passing signals through and from a subsystem. Dragging ports from Origins but Sinks folders generates inputs and outputs. The interfaces mostly on external (parent) block were generated automatically as they are generated throughout the subsystem. Each parent system is added to the controller by adding the necessary signals.

7.6 Setting Simulation Parameters:

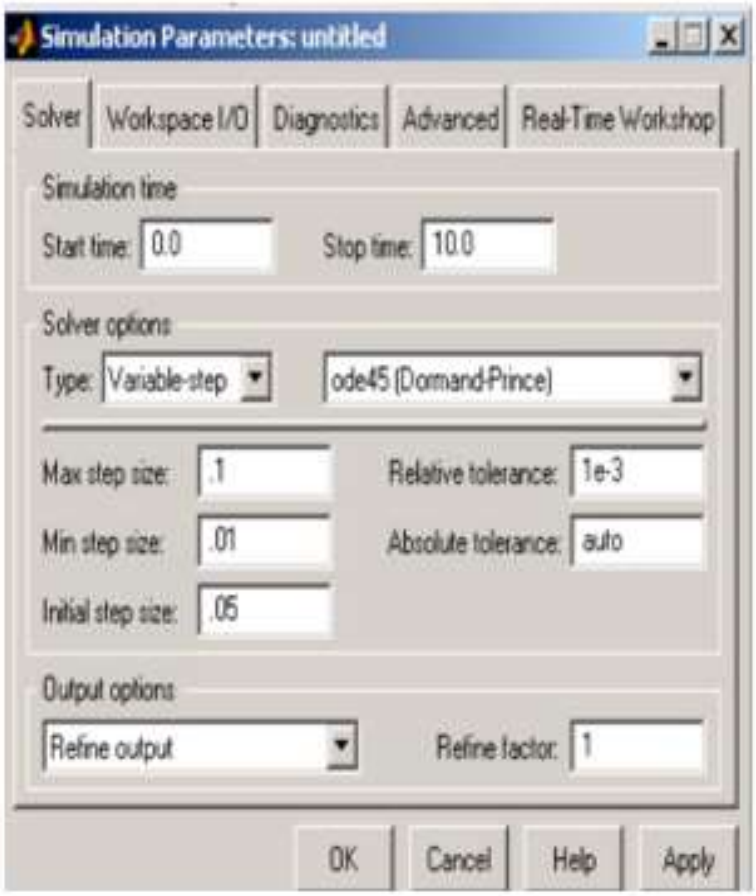

Figure 7.3: Setting of simulation parameters

A number technology to overcome any differential equation is often needed to run another simulation mostly on machine. The device may be replicated mostly on blocks within as just a continuous machine or a separate method. The starting and end period of the simulation may be set.

The lowest and highest step size could be specified throughout case of nonlinear step size. The set phase size is suggested which enables the information technology project to also be indexed to a particular number of pixels. Depending on the device parameters, the design phase size must be determined. A thermal cycle can take a couple of minutes, however a DC engine in the device can be very fast and take several milliseconds phase.

7.7 Simulation Diagrams and Results:

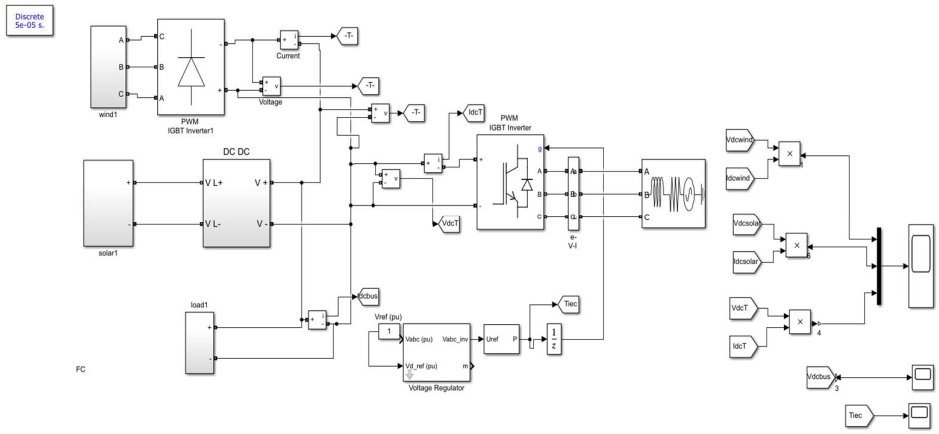

Fig.7. 4. Scenario 1: DC microgrid with microturbine, fuel cell and load.

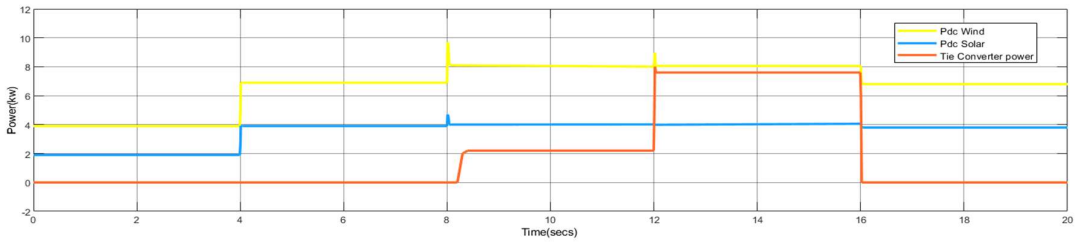

(a)

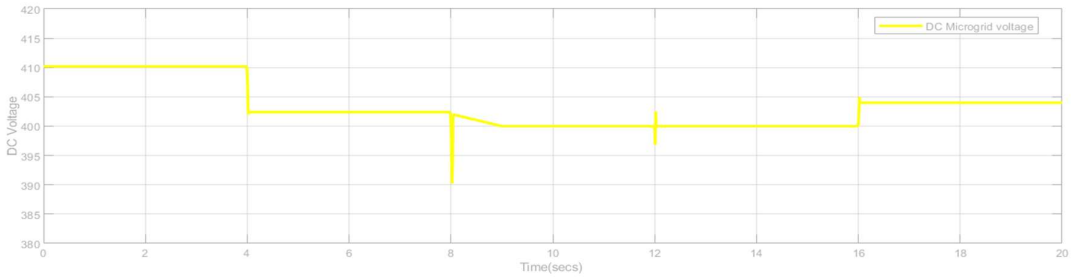

(b)

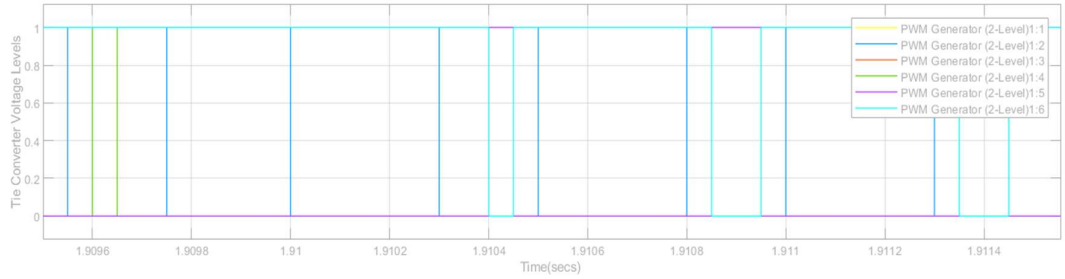

(c)

Fig. 7.5. Scenario 1: Results showing (a) generators and tie-converter power, (b) DC microgrid voltage and (c) tie-converter control signals for four different load operating conditions.

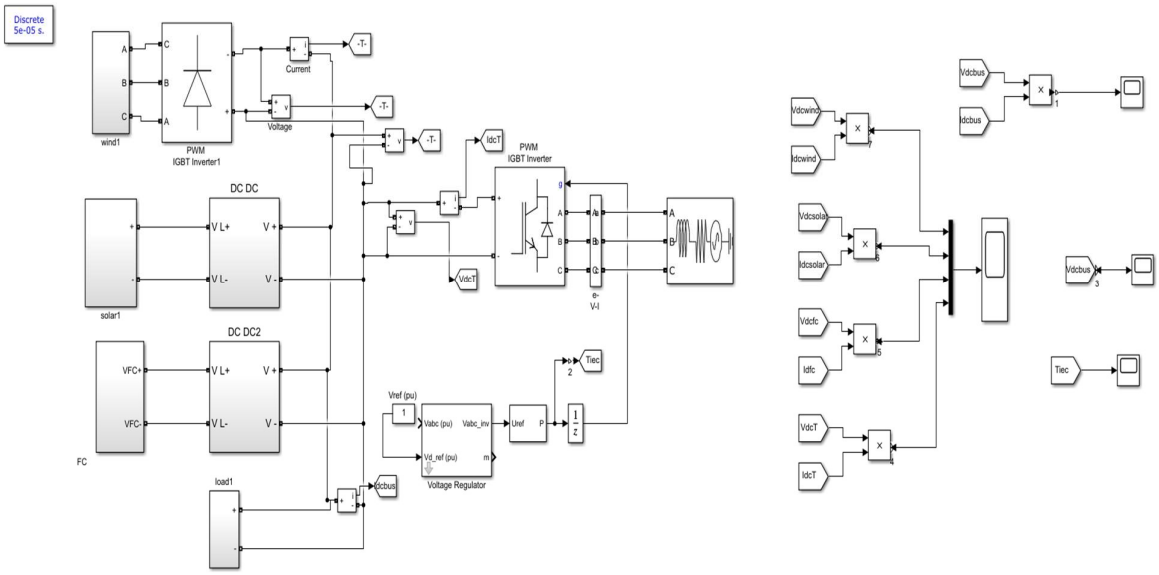

Fig.7. 6. Scenario 2: DC microgrid with microturbine, fuel cell, solar PV and load

.

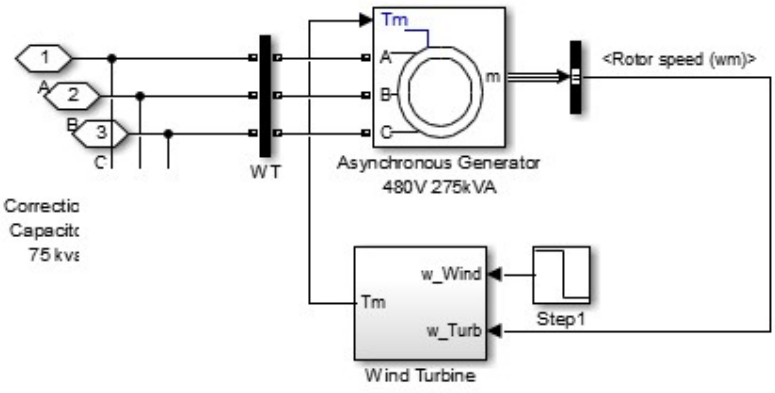

Fig7.7: (a)Wind subsystem

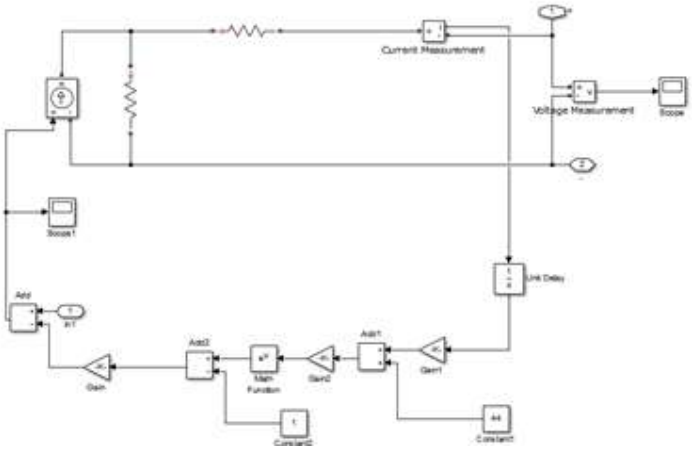

(b) Simulation diagram of Pv subsystem

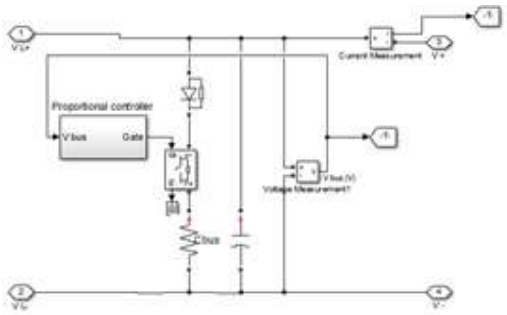

(c)Simulation diagram of dc-dc

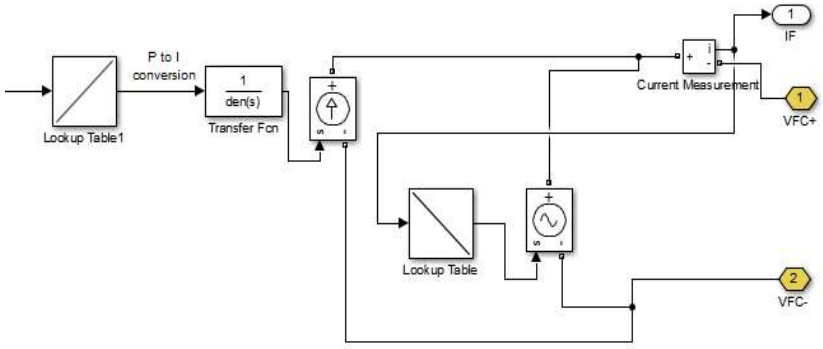

Fig(d): Modelling of fuel cell Fuel cell

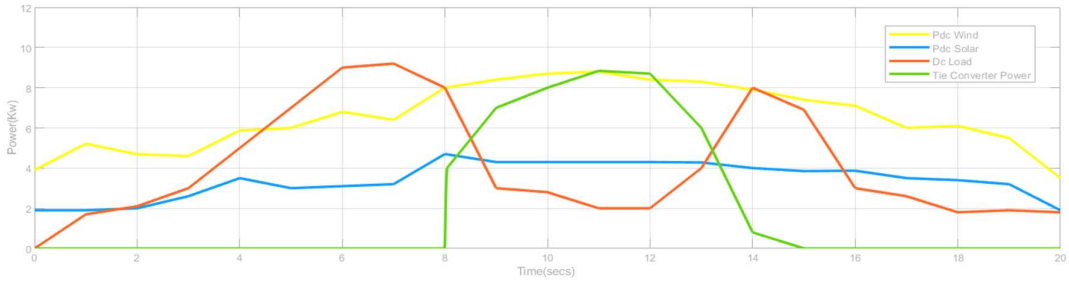

(a)

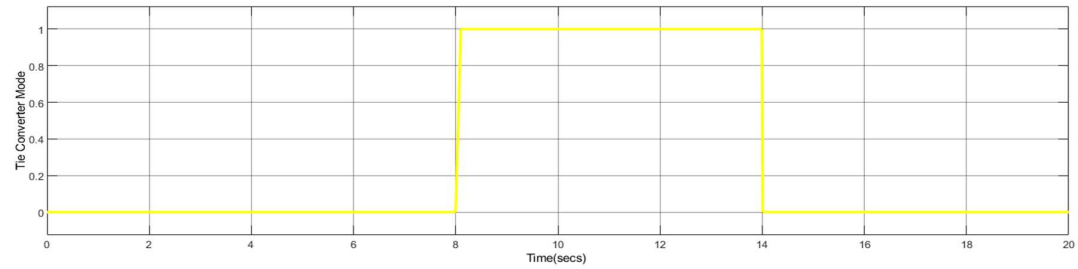

(b)

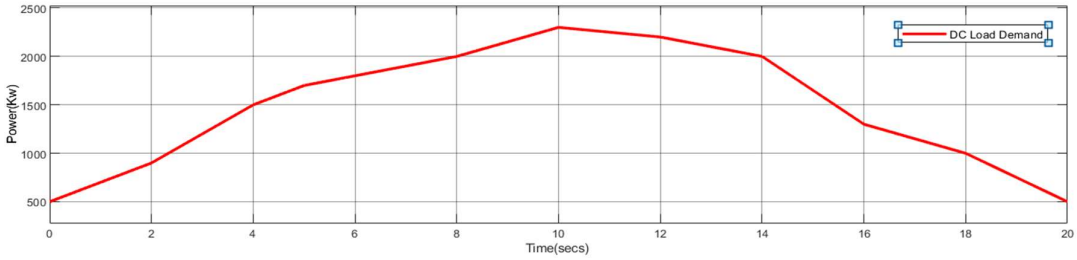

(c)

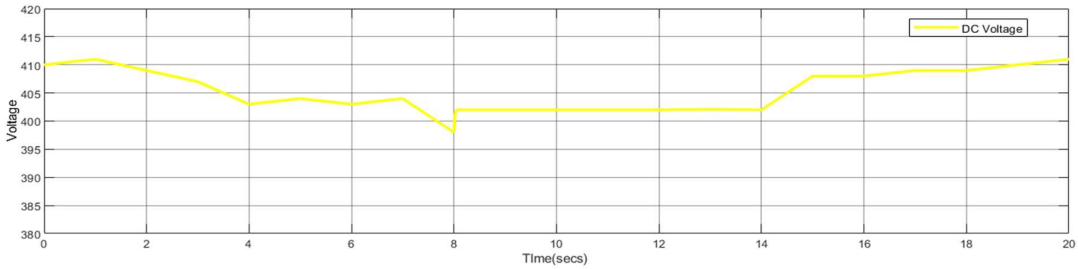

(d)

Fig. 7.8. Scenario 2: Results showing (a) DC microgrid load demand, (b) generators and tie-converter power, (c) DC microgrid voltage and (d) tie-converter control signals at varying solar PV and load operating conditions.

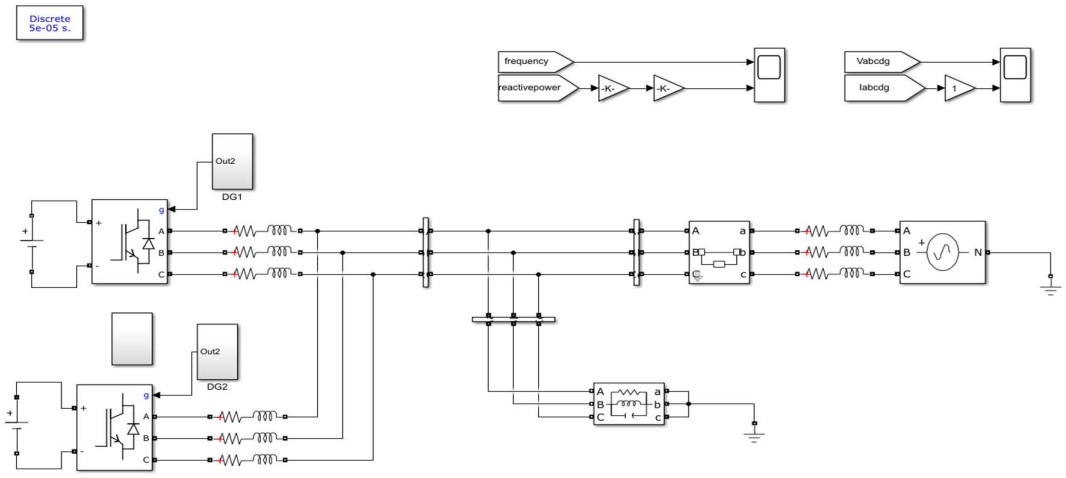

Fig 7.9. Simulation configuration of the islanding detection method

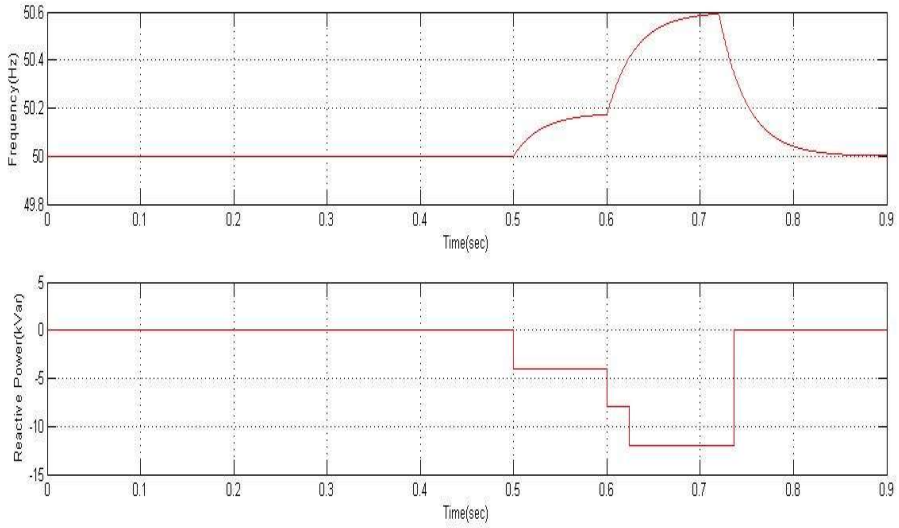

Fig 7.10. shows Reactive power and frequency vs time in sec

CONCLUSION

An autonomous power management scheme has been presented for interlinked AC-DC micro grids having different configurations. The proposed scheme manages the power deficit in the DC micro grid efficiently and autonomously. The number of tie-converters in operation has been reduced with the proposed prioritization to avoid unnecessary operational losses. The scheme has demonstrated better voltage regulation in the DC micro grid. The performance and robustness of the proposed scheme have been validated for two different scenarios of the DC micro grid at variable load conditions.

REFERENCES

[1] J. Rocabert, A. Luna, F. Blaabjerg, and P. Rodr´ıguez, “Control of power converters in AC microgrids,” *IEEE Transactions on Power Electronics*, vol. 27, no. 11, nov-2011

[2] M. Liserre, T. Sauter, and J. Y. Hung, “Future energy systems: integrating renewable energy sources into the smart power grid through industrial electronics,” *IEEE Industrial Electronics Magazine*, vol.4. no. 1, pp. 18–37, Mar. 2010.

[3] M. Tsili and S. Papathanassiou, “A review of grid code technical requirements for wind farms,” *IET Renewable Power Generation*, vol. 3, no. 3, pp. 308–332, Sep. 2009.

[4] T. Strasser, F. Andren, J. Kathan, C. Cecati, C. Buccella, P. Siano, P. ´ Leitao, G. Zhabelova, V. Vyatkin, P. Vrba, and V. Ma ˇ ˇ r´ık, “A review of architectures and concepts for intelligence in future electric energy systems,” *IEEE Transactions on Industrial Electronics*, vol. 62, no. 4, pp. 2424–2438, Apr. 2015.

[5] A. Kwasinski, “Quantitative evaluation of dc microgrids availability: Effects of system architecture and converter topology design choices,” *IEEE Transactions on Power Electronics*, vol. 26, no. 3, pp. 835–851, Mar. 2011.

[6] P. Basak, S. Chowdhury, S. H. N. Dey, S. P. Chowdhury, “A literature review on integration of distributed energy resources in the perspective of control, protection and stability of microgrid,” *Renewable and Sustainable Energy Reviews*, vol. 16, no. 8, pp. 5545–5556, Oct. 2012.

[7] D. E. Olivares, A. Mehrizi-Sani, A. H. Etemadi, C. A. Canizares, R. Iravani, M. Kazerani, A. H. Hajimiragha, O. Gomis-Bellmunt, M. Saeedifard, R. alma-Behnke, G. A. Jimenez-Estevez, and N. D. Hatziargyriou, “Trends in microgrid control,” *IEEE Transactions on Smart Grid*, vol. 5, no. 4, pp. 1905–1919, Jul. 2014.

[8] N. Hatziargyriou, H. Asano, R. Iravani, and C. Marnay, “Microgrids,” *IEEE Power and Energy Magazine*, vol. 5, no. 4, pp. 78–94, Jul. /Aug. 2007.

[9] L. E. Zubieta, “Are microgrids the future of energy?: DC microgrids from concept to demonstration to deployment,” *IEEE Electrification Magazine*, vol. 4, no. 2, pp. 37–44, Jun. 2016.

[10] G. Venkataramanan and C. Marnay, “A larger role for microgrids,” *IEEE Power and Energy Magazine*, vol. 6, no. 3, pp. 78–82, May-Jun. 2008.

[11] W. Yuan, J. H. Wang, F. Qiu, C. Chen, C. Q. Kang, and B. Zeng, “Robust optimization-based resilient distribution network planning against natural disasters,” *IEEE Transactions on Smart Grid*, vol. 7, no. 6, pp. 2817–2826, Nov. 2016.

[12] N. Nikmehr, S. N. Ravadanegh, "Optimal power dispatch of multimicrogrids at future smart distribution grids," *IEEE Transactions on Smart Grid*, vol. 6, no. 4, pp. 1648–1657, Jul. 2015.

[13] H. Farzin, M. Fotuhi-Firuzabad, M. Moeini-Aghtaie, "Enhancing power system resilience through hierarchical outage management in multimicrogrids," *IEEE Transactions on Smart Grid*, vol. 7, no. 6, pp. 2869– 2879, Nov. 2016.

[14] J. Wu, X. H. Guan, "Coordinated multi-microgrids optimal control algorithm for smart distribution management system," *IEEE Transactions on Smart Grid*, vol. 4, no. 4, pp. 2174–2181, Dec. 2013.

[15] N. Hatziargyriou, "Operation of multi-microgrids," in *Microgrids: Architectures and Control*, Wiley-IEEE Press, 2014.

[16] I. U. Nutkani, P. C. Loh, and F. Blaabjerg, "Distributed operation of interlinked AC microgrids with dynamic active and reactive power tuning," *IEEE Transactions on Industry Applications*, vol. 49, no. 5, pp. 2188–2196, Sep. /Oct. 2013.